Bulletin of the
Association of Engineering Geologists
Vol. XXIII, No. 2, 1986
pp. 139–165

Origin of Land Subsidence and Earth Fissuring, Northeast Phoenix, Arizona

MICHAEL K. LARSON*
TROY L. PÉWÉ
Department of Geology, Arizona State University, Tempe, AZ 85287

ABSTRACT

Differential subsidence over a buried bedrock hill caused by rapid water-level decline resulted in a 400-ft (120 m) long earth fissure in a northeast Phoenix construction site in January, 1980. This is the first occurrence in the Paradise Valley basin, and the first within the city of Phoenix.

Local water levels have declined more than 300 ft (90 m) accompanied by 3.44 ft (1.05 m) of measured subsidence, with indirect evidence for 5 ft (1.5 m). The depth to ground water is as much as 580 ft in the area. The maximum subsidence rate measured was 0.44 ft. (0.13 m) annually. Water levels began dropping in the mid-1950's, and subsidence began a decade later after 100 to 150 ft (30 to 45 m) of decline in water level. The subsidence bowl has grown about 2 mi^2 (5 km^2) annually, first mostly westward, and more recently north and east, with further expansion expected. More than 9 ft (3 m) of subsidence is possible.

Gravity survey results suggest the fissure is associated with a bedrock hill buried at 150 ft (45 m) on a large pediment. Measured differential subsidence, after fissuring, occurred in a pattern similar to the inferred subsurface bedrock configuration, indicating that the fissure was coincident with surficial horizontal tensile maxima above the crest of the buried hill. Maximum annual strain and accumulated tensile strain at the time of fissuring were calculated at 0.01 percent and 0.06 percent, respectively. These data suggest future reactivation of the filled-in fissure, and on the basis of gravity measurements, probable lengthening of the fissure. Finite element analysis indicates maximum surficial tensile stress of 3,400 psf (1.4 kg/cm^2) and strain of 0.19 percent when fissuring occurred.

The large pediment that underlies most of the study area is divided into a shallow inner part [less than 500 ft (150 m) deep] of moderate relief; and a deeper, outer part gently sloping northeastward from 500 to 1,000 ft (150 to 300 m). The pediment is separated from thick alluvial deposits toward the center of the valley by a major NW–SE normal fault. This subsurface configuration controls the spatial pattern of land subsidence, water-level decline, and future fissuring. Fissures may be localized in three geologic settings: 1) buried bedrock hills, 2) the hinge-line of subsiding areas, and 3) buried faults.

* Present address: Kansas Department of Health and Environment, Oil Field and Environmental Geology Section, 1014 Cody, Hays, KS 67601.

517.004

Bulletin of the
Association of Engineering Geologists
Vol. XXIII, No. 2, 1986
pp. 139–165

Origin of Land Subsidence and Earth Fissuring, Northeast Phoenix, Arizona

MICHAEL K. LARSON*
TROY L. PÉWÉ
Department of Geology, Arizona State University, Tempe, AZ 85287

ABSTRACT

Differential subsidence over a buried bedrock hill caused by rapid water-level decline resulted in a 400-ft (120 m) long earth fissure in a northeast Phoenix construction site in January, 1980. This is the first occurrence in the Paradise Valley basin, and the first within the city of Phoenix.

Local water levels have declined more than 300 ft (90 m) accompanied by 3.44 ft (1.05 m) of measured subsidence, with indirect evidence for 5 ft (1.5 m). The depth to ground water is as much as 580 ft in the area. The maximum subsidence rate measured was 0.44 ft. (0.13 m) annually. Water levels began dropping in the mid-1950's, and subsidence began a decade later after 100 to 150 ft (30 to 45 m) of decline in water level. The subsidence bowl has grown about 2 mi^2 (5 km^2) annually, first mostly westward, and more recently north and east, with further expansion expected. More than 9 ft (3 m) of subsidence is possible.

Gravity survey results suggest the fissure is associated with a bedrock hill buried at 150 ft (45 m) on a large pediment. Measured differential subsidence, after fissuring, occurred in a pattern similar to the inferred subsurface bedrock configuration, indicating that the fissure was coincident with surficial horizontal tensile maxima above the crest of the buried hill. Maximum annual strain and accumulated tensile strain at the time of fissuring were calculated at 0.01 percent and 0.06 percent, respectively. These data suggest future reactivation of the filled-in fissure, and on the basis of gravity measurements, probable lengthening of the fissure. Finite element analysis indicates maximum surficial tensile stress of 3,400 psf (1.4 kg/cm^2) and strain of 0.19 percent when fissuring occurred.

The large pediment that underlies most of the study area is divided into a shallow inner part [less than 500 ft (150 m) deep] of moderate relief; and a deeper, outer part gently sloping northeastward from 500 to 1,000 ft (150 to 300 m). The pediment is separated from thick alluvial deposits toward the center of the valley by a major NW–SE normal fault. This subsurface configuration controls the spatial pattern of land subsidence, water-level decline, and future fissuring. Fissures may be localized in three geologic settings: 1) buried bedrock hills, 2) the hinge-line of subsiding areas, and 3) buried faults.

* Present address: Kansas Department of Health and Environment, Oil Field and Environmental Geology Section, 1014 Cody, Hays, KS 67601.

INTRODUCTION

Earth fissures, which are long, narrow, eroded tension cracks associated with land subsidence caused by ground-water withdrawal, have formed during the past 50 years in alluvial basins of southern and south-central Arizona. Until recently, the fissure hazard has been confined to outlying agricultural areas. In January, 1980, a fissure opened in a residential construction site in northeast Phoenix. This fissure is the first known occurrence in the Paradise Valley basin, and within the city of Phoenix.

Land subsidence and earth fissures pose serious problems for urban areas, with the potential for widespread damage to manmade structures. Some of the most important parts of the municipal infrastructure are the most vulnerable. Water-well failure is a dramatic manifestation of subsidence as the casing collapses or the well-head protrudes above the ground. Aqueducts designed for gravity flow may overflow as a result of local sags and gradient reversals. Storm drains and sewer mains that also depend on gravity flow may reverse flow or clog because of altered gradients, and in extreme cases rupture. Subsidence may also necessitate new designs of storm drainage systems, and expensive repeated levelings of benchmarks where surveying data are quickly made obsolete. Fissures may directly damage buildings, roads, and other architectural structures, and even without ground failure, differential subsidence in and of itself may cause damage to structures which are large in area or height.

Purpose and Scope

The objectives of this study were to investigate land subsidence, causes of the fissure in northeast Phoenix, and to determine the relationship of subsurface bedrock topography to fissuring. A detailed gravity survey, supplemented by geologic mapping, precise repeated land surveying, and interpretation of well records in the vicinity of the fissure constituted the basis for geologic and hydrologic interpretation. Based on the ground-water history and inferred subsurface bedrock configuration of the area, general predictions of future fissuring were made. Because there is a high potential for damage in an urbanized area, this study may aid in minimizing problems associated with fissuring.

Geographic Setting

The study area covers part of the western margin of Paradise Valley, a deep alluvial basin in the Basin-and-Range physiographic province and part of the adjacent Phoenix Mountains (Figure 1). Most of the area lies within the city of Phoenix, but some of it is included in the city of Scottsdale and the town of Paradise Valley. Rapid development of the area, which is predominantly residential, has occurred during the past 20 years.

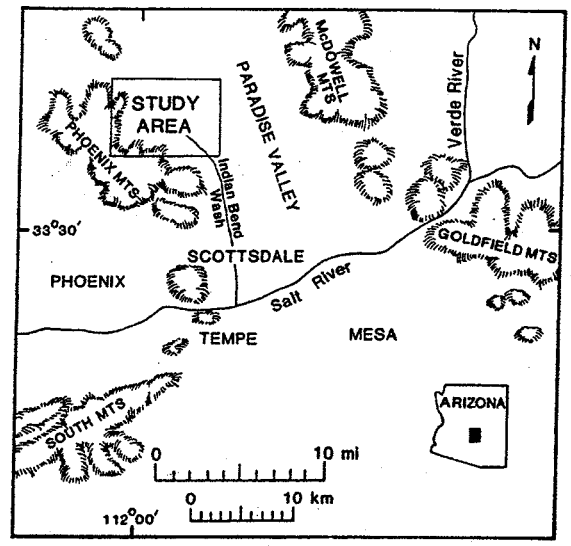

Figure 1. Index map showing location of study area.

Regional Geology

Late-Tertiary Basin-and-Range block faulting in the region resulted in linear mountain ranges and intervening narrow elongate sediment-filled basins. Sedimentation in Paradise Valley has filled the basin and buried some low hills and pediments on the upthrown fault block (Phoenix Mountains). The gently sloping floor of Paradise Valley is broken by small, isolated bedrock hills near the margins of the surrounding mountains. The basin-fill material is typically poorly sorted, unconsolidated fine to coarse-grained sediments.

The Phoenix Mountains consist of Precambrian schist, phyllite, quartzite, and amphibolite, and Tertiary basalt and conglomerate. Precambrian metamorphic rocks display a prevailing northeast-striking foliation that dips steeply to the southeast (Wilson et al., 1957; Shank and Péwé, 1973; and Cordy et al., 1977).

Previous Work

Paradise Valley was included in early reconnaissance geologic and hydrologic reports (Davis, 1897; Lee, 1905; Meinzer and Ellis, 1915; and McDonald et al., 1947). Arteaga and others (1968) documented the historical ground-water development that led to the present overdraft of supplies in Paradise Valley.

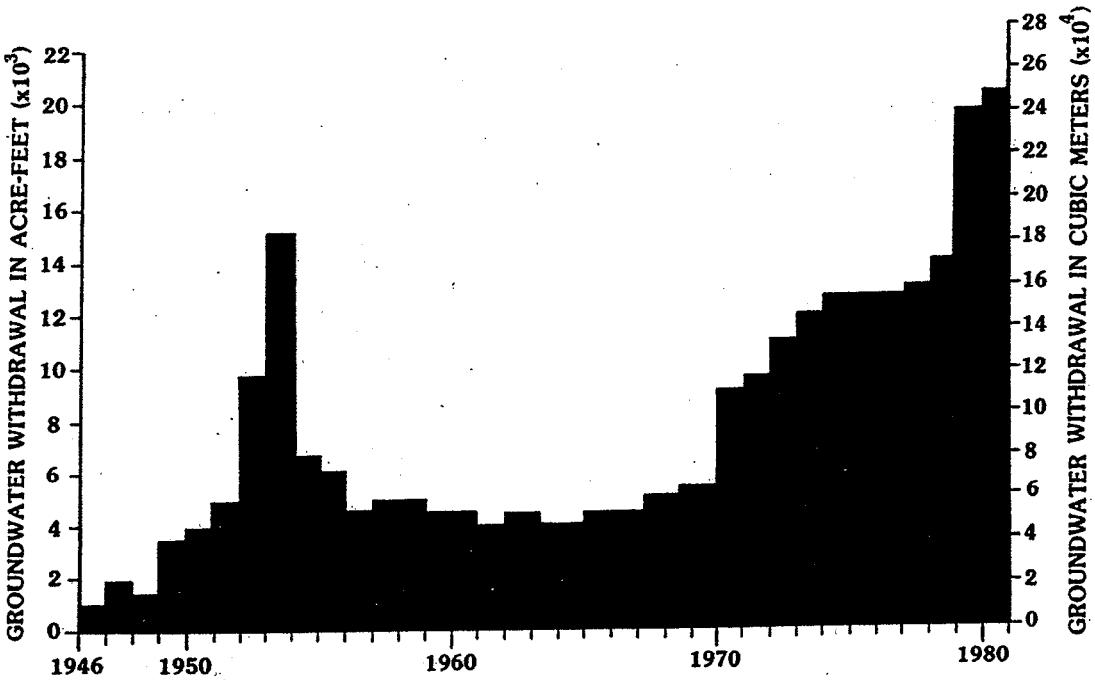

Figure 2. Estimated annual ground-water withdrawals, central Paradise Valley, Arizona (1946–1980). (Sources: Arteaga et al., 1968; U.S. Geological Survey, Phoenix Office, unpublished data; Arizona Department of Water Resources, unpublished data).

As part of environmental geology studies, the geology of the Phoenix Mountains was mapped by Shank and Péwé (1973) and the Paradise Valley quadrangle by Cordy and others (1977).

Peterson (1968) conducted a gravity survey over a large area of south-central Arizona that included northeast Phoenix, and a later more detailed gravity survey by Lausten (1973) covered the entire Paradise Valley basin. Lausten concluded that fissures may form over buried fault scarps inferred over areas of steep gravity gradients. Several investigators suggested fissures may form in Paradise Valley near areas of rapid ground-water withdrawal along the margins of the basin (Christenson and Péwé, 1978; Welsch and Péwé, 1979; Cordy et al., 1977; and Bales et al., 1980).

HYDROLOGY

Historical Background

During the past century, ground-water use has increased in south-central Arizona due to expanded agricultural and urban development. Diversion of surface water for irrigation prior to 1920 caused a rise in water levels to the extent that some areas were waterlogged. During the early 1950's, water levels began to drop rapidly because of increased pumping. The average annual consumption of ground water from 1952 to 1964 in the Salt River Valley was estimated at 1,718,000 acre-feet (2,118 m^3) while the average annual supply is only 789,000 acre-feet (972 m^3) (U.S. Department of the Interior, Bureau of Reclamation, 1976). This overdraft of 929,000 acre-feet (1,145 m^3) per year has caused water-level declines greater than 300 ft (90 m) in several areas (Laney et al., 1978).

In the late 1880's, Paradise Valley was viewed with great potential as irrigated farmland to be served by water diverted through a canal from the Verde River; however, the project was never completed because of litigation over water rights (Meinzer and Ellis, 1915). Unlike irrigated areas of the southern part of Paradise Valley, where surface water is supplied by the Salt River Project, minimal ground-water resources restricted agricultural developments in the study area in central Paradise Valley. With urban expansion in central Paradise Valley and addition of deep, large-capacity private and municipal wells since the early 1950's, ground-water withdrawal has been greatly increased. (Figure 2).

Local Conditions

Ground water is principally withdrawn from unconsolidated alluvium in Paradise Valley. The alluvium is generally less than 1,000 ft (300 m) thick over most of the study area, and estimated to exceed 9,000 ft (2,700 m) near the center of the basin (Lausten, 1974). Sediments, typically poorly sorted, are

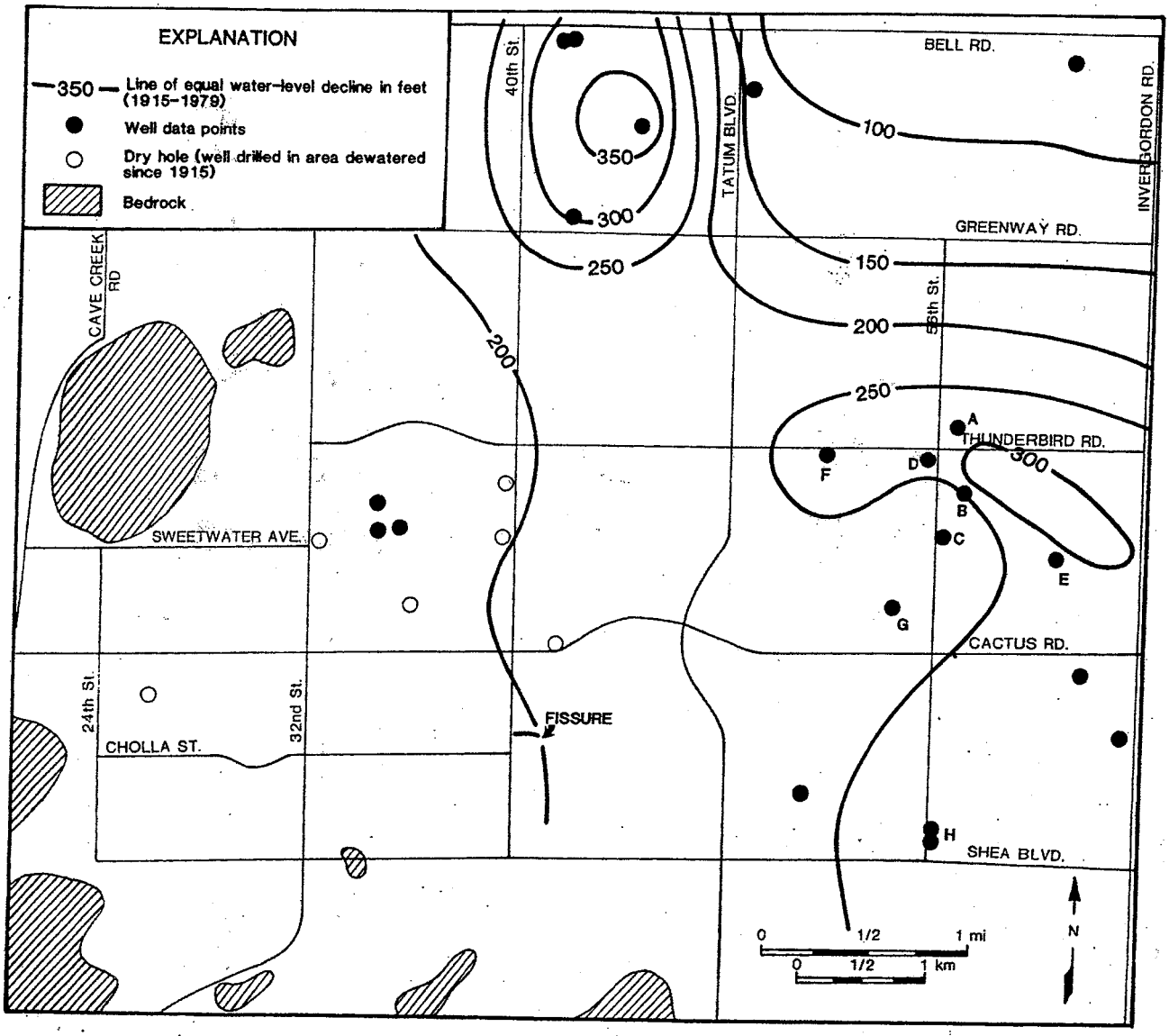

Figure 3. Decline in water-levels in feet, northeast Phoenix, Arizona (1915–1979). (See Figure 5 for water-level hydrographs of lettered well data points.) Sources: Meinzer and Ellis, 1915; McDonald et al., 1947; and Arteaga et al., 1968; City of Phoenix Water Production Office unpublished data; U.S. Geological Survey, Phoenix office, unpublished data; Arizona Department of Water Resources, unpublished data.

dominantly fine-grained clays and silts intercalated with sandy and gravelly layers. Unconfined aquifer conditions exist over most of the area, but near the northern boundary of the study area, a confined aquifer is separated from the overlying unconfined aquifer by a clay layer more than 200 ft (60 m) thick. Well logs in the area reveal an indurated low-porosity conglomerate that underlies unconsolidated alluvium, presumably equivalent to outcrops of Tertiary age conglomerate in the Phoenix Mountains. Fractured zones in the conglomerate yield abundant water in some areas (Daly, 1982).

Most water stored in the Paradise Valley basin accumulated within the past several thousand years slowly recharged via runoff from Indian Bend Wash and other mountain washes, and to a lesser extent, seepage of rainfall on the valley floor. Ground water flows southward toward the Salt River in the area, except where now interrupted by two 'cones of depression' of the water table, where water levels

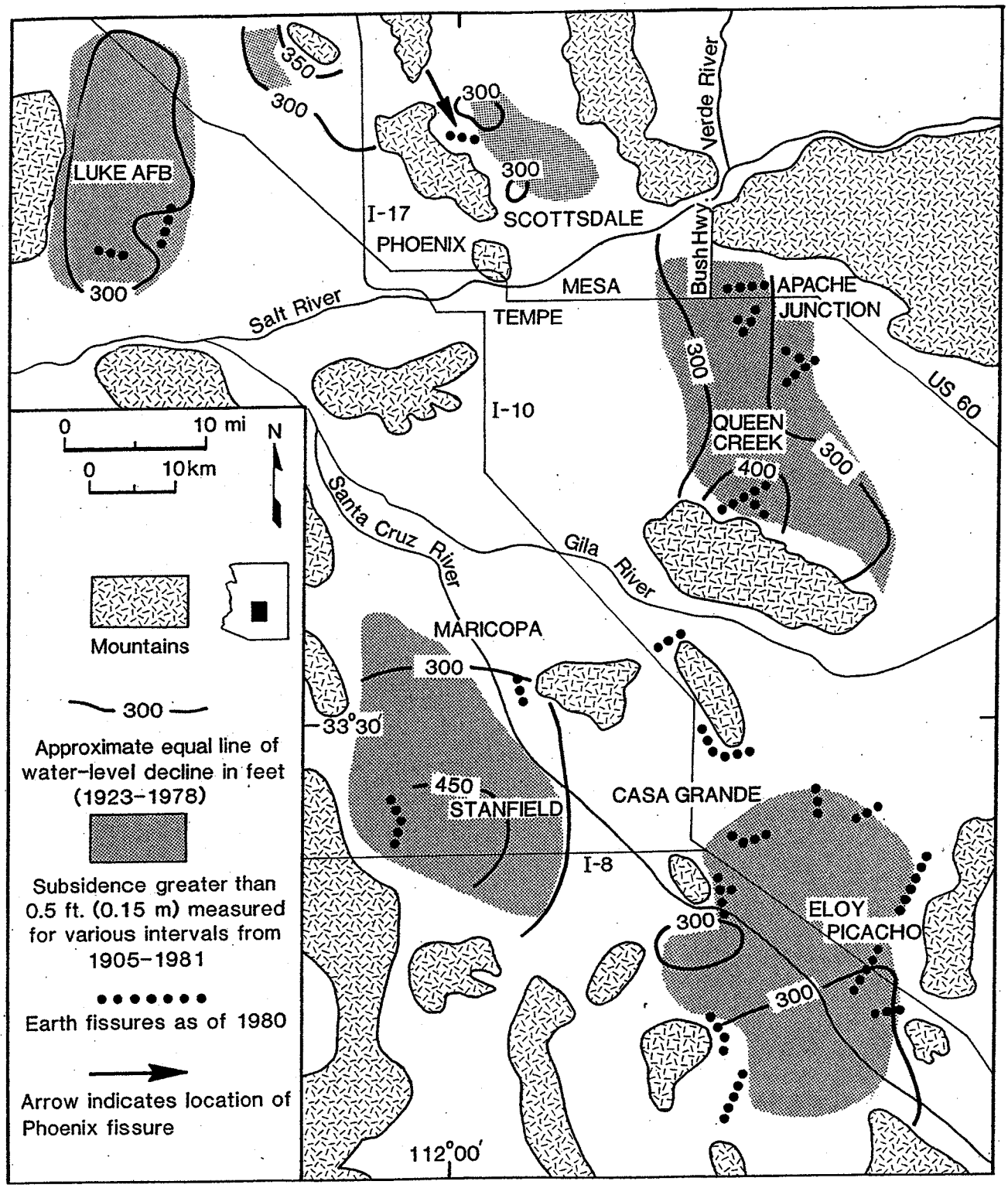

Figure 4. Water-level declines, land subsidence, and earth fissures in south-central Arizona. (Sources: Schumann, 1974; Winikka and Wold, 1976; and Laney et al., 1978; Arizona Department of Transportation, 1981; Larson, 1982a.)

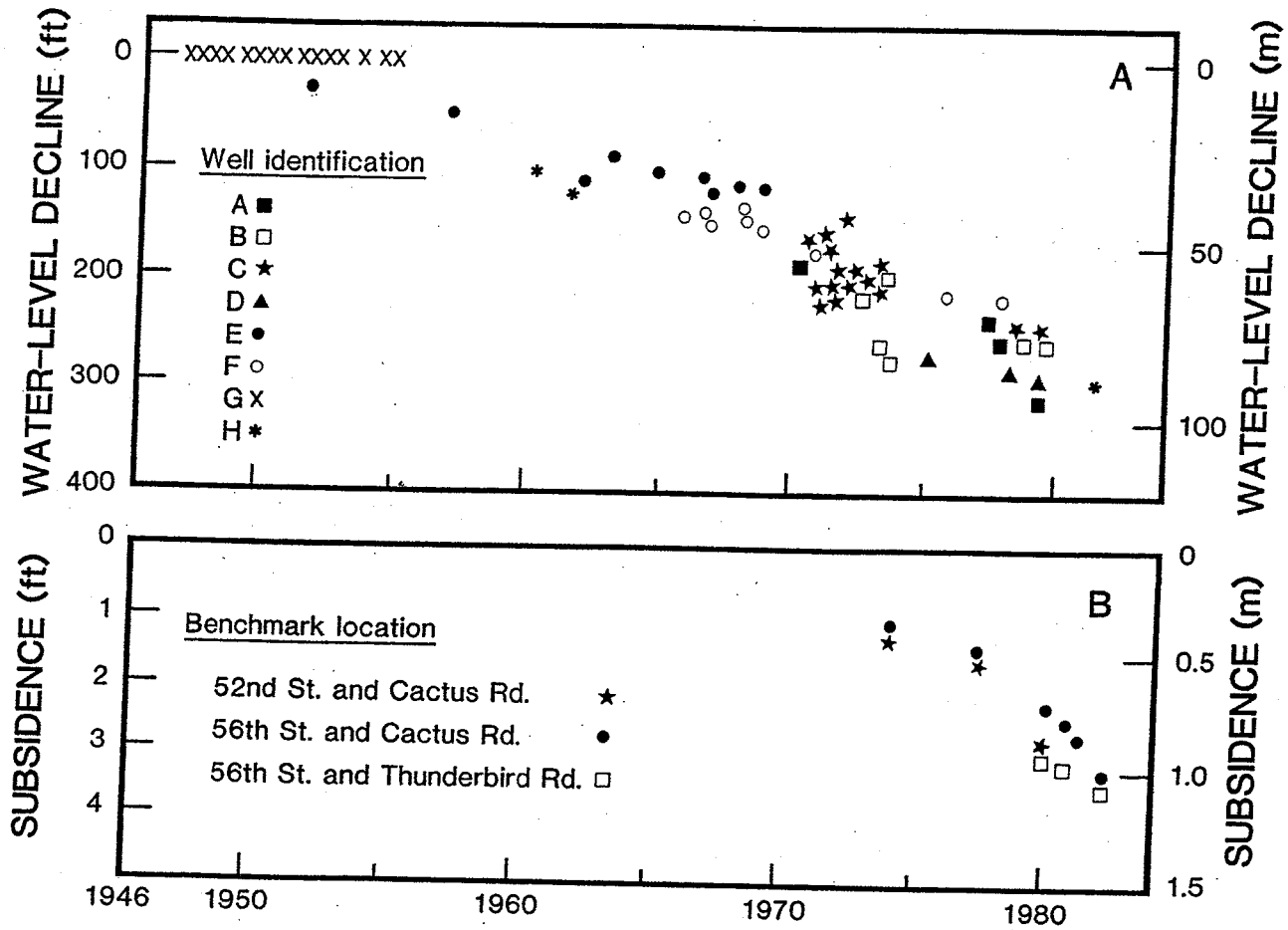

Figure 5. Composite water-level hydrographs and subsidence of selected benchmarks in southern cone of depression of water levels (1946–1982). A) Composite water-level hydrograph in southern cone of depression (see Figure 3 for well locations). B) Subsidence histories of selected benchmarks in southern cone of depression of water levels. Exact dates of original levelings not known, however, the original measurements are known to be pre-1965. (Sources: City of Phoenix Engineering Department, Survey Division, unpublished data; City of Phoenix Water Production Office, unpublished data; U.S. Geological Survey, Phoenix office, unpublished data.)

are as much as 580 ft (175 m) deep. The cones of depression appear to be caused by two municipal well-fields. Water levels remained nearly constant in the study area prior to about 1950, generally within 250 ft (75 m) of the surface (Meinzer and Ellis, 1915; McDonald et al., 1947). Increased pumpage in relatively unproductive aquifers has caused rapid water-level decline, particularly in two areas where ground water has dropped more than 300 ft (90 m) from its original level (Figure 3). Withdrawals of ground water exceed the natural recharge rate many times, and this severe overdraft has resulted in depletion of thin aquifers peripheral to the mountains, and loss of supply to shallow wells. More wells will certainly become dry as heavy pumping in the area continues.

LAND SUBSIDENCE

General Statement

Land subsidence is a geological phenomenon caused by a variety of natural and manmade processes. A common cause of man-induced land subsidence is fluid withdrawal, and for purposes of this study only the effects of ground-water withdrawal need be considered since oil and gas do not occur in this area.

Measured compaction in deep wells near Eloy and Apache Junction, in south-central Arizona, indicates most of the measured land subsidence compaction may be attributed to compaction of the upper 1,000 to 1,500 ft (300 to 450 m) of sediments (Schumann and Poland, 1969; Raymond, 1980).

Subsidence per unit water-level decline has been observed to markedly increase after water levels have declined past a certain threshold value. This threshold is related to the natural pre-consolidation stress of deposits before man-induced water-level declines began, and for alluvial basins of southern Arizona, the value is approximately 100 to 150 ft (30 to 45 m) (Holzer, 1981).

Subsidence in South-Central Arizona

Subsidence in south-central Arizona was first detected near Eloy in the Picacho Basin in 1948 (Schumann and Poland, 1969) (Figure 4). Repeated precise leveling has indicated as much as 12.5 ft (3.8 m) of subsidence near Eloy (Laney et al., 1978). The spatial and temporal distribution of subsidence correlates to the historical pattern of water-level declines. Subsidence rates have varied, with a maximum value of 0.560 ft (0.170 m) per year documented from 1952 to 1964 (Schumann and Poland, 1969).

Within the Salt River Valley, subsidence data is mostly of a reconnaissance nature. In areas of greatest decline in water levels, large elevational differences have been detected by first- and second-order relevelings by the U.S. Coast and Geodetic Survey (now the National Geodetic Survey) during the period from 1933 to 1981 (Elliott, 1969; Arizona Department of Transportation, 1981). Preliminary adjustment of the most recent leveling in 1981 reveals that the maximum measured subsidence of a benchmark is 5.1 ft (1.6 m) near U.S. Highway 60 and the Bush Highway in east Mesa, from 1948 to 1981 (Figure 4), and during the same interval, probably 6.3 ft (1.9 m) of subsidence has occurred at a nearby intersection (Arizona Department of Transportation, 1981).

Subsidence in Northeast Phoenix

The onset of land subsidence in northeast Phoenix is not known; however, it probably began during the late 60's or early 70's in response to falling water levels. Records furnished by the Survey Section of the City of Phoenix Engineering Department for benchmarks span various time intervals from 1965 to 1982 (Larson, 1982b). Recent subsidence monitoring has all been tied to stable benchmarks (Péwé and Larson, 1982). To supplement the history of surveyed benchmarks, subsidence was also evaluated by detailed relevelings of gravity stations near the fissure during a twelve-month period (April 1981–1982), and by comparing elevational differences between city-surveyed gravity stations of this study. According to U.S. Geological Survey standards for topographic maps, spot and interpolated elevations on slopes less than 15 percent are correct to within one-quarter of the contour interval (Marsden, 1960). Because the contour interval in the study area is 10 ft (3 m), and most stations are at a consistent curb height above the street, differences derived by this method should be accurate to within 2.5 ft (0.76 m).

A comparison of subsidence plots with hydrographs of wells indicates subsidence began when water levels declined approximately 100 to 150 ft (30 to 45 m) from their original levels (Figure 5). Subsidence probably began about 1965 in the vicinity of 52nd Street and Thunderbird Road (Figure 6A). Since 1970, the subsidence bowl then increased in size at an average rate of 2 mi^2 (5 km^2) per year. Early expansion of the subsidence bowl was predominantly in a westerly direction (Figure 6A, B), with more recent expansion toward the north and east (Figure 6C, D). The area west of 32nd Street has remained stable.

The center of the subsidence bowl in 1982 (Figure 6D) was approximately one mi (1.6 km) west of the center of the southern cone of depression of water levels (Figure 3). This relationship probably reflects an earlier pumping and subsidence history to the west, or possibly is due to variations in material properties of alluvium or the asymmetry of groundwater flow. Little subsidence has been measured near the northern cone of depression of water levels, presumably because of low permeability of the thick clay layer. Differences in total subsidence are apparently a function of the differences in subsidence rate and the total time since settlement began for different areas. Based on a comparison of elevation data compiled on 1962 U.S. Geological Survey topographic maps with a leveling of city benchmark and gravity stations in 1980, about 5 ft (1.5 m) of total subsidence is suggested for 52nd Street and Sweetwater Avenue; this is approximately the inferred center of subsidence (Figure 6D).

Near the center of the subsidence bowl near 56th Street, total subsidence measured between 1965 and March, 1982 along 56th Street is 3.44 ft (1.05 m) at Thunderbird Road, and 3.35 ft (1.02 m) at Cactus Road (Figure 5B). The subsidence rate has increased at Cactus Road and 56th Street from 0.16 ft (0.05 m) per year (1974 to 1977) to 0.36 ft (0.12 m) per

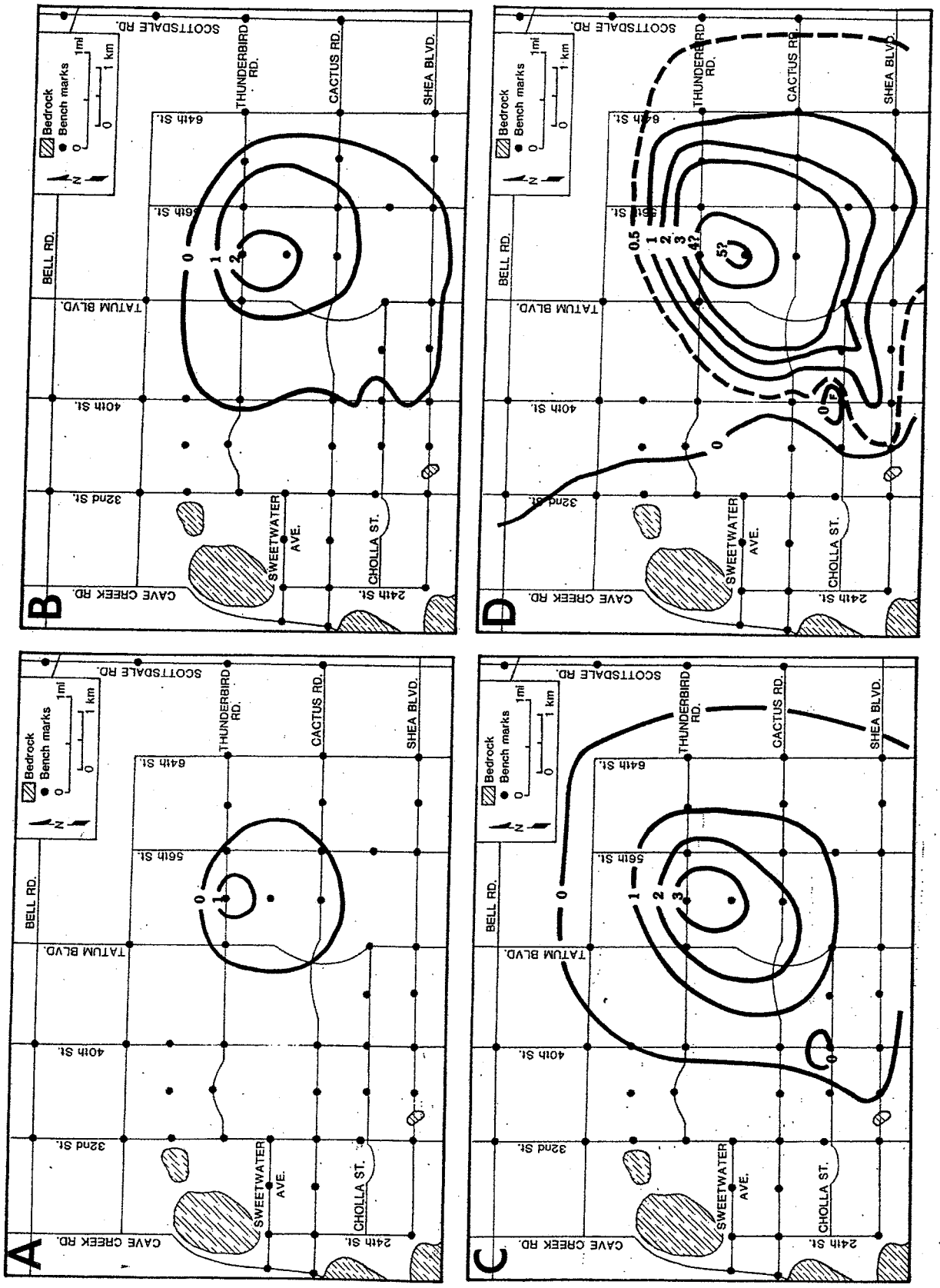
A
B
C
D
Bedrock
Bench marks
0
1 mi
1 km
N
SCOTTSDALE RD.
THUNDERBIRD RD.
CACTUS RD.
SHEA BLVD.
64th St.
56th St.
BELL RD.
TATUM BLVD.
40th St.
32nd St.
SWEETWATER AVE.
CHOLLA ST.
CAVE CREEK RD.
24th St.
0
1
2
3
0.5
4?
5?

year (1979 to 1982). During the most recent measurement interval (September 1980 to February 1982), a subsidence rate of 0.44 ft (0.15 m) per year has been noted. Because of the increased subsidence rate at Cactus Road and 56th Street, and a rapid subsidence rate of 0.34 ft (0.10 m) per year (1981–1982) at Tatum Boulevard and Cholla Street (Figure 6D), it is possible that a southward shift in the center of the subsidence bowl has occurred. One instance of well-casing failure possibly caused by subsidence has been reported in the area (Well H on Figure 3) (Daly, 1982).

EARTH FISSURES

Earth fissures are widespread in southern and south-central Arizona (Figure 4). The first fissure was observed near Picacho in 1927 (Leonard, 1929). Since the late 1940's, accelerated ground-water withdrawal has caused intense fissuring of several alluvial basins.

Fissures occur in unconsolidated sediments, typically near the margins of alluvial valleys or near outlying bedrock outcrops where ground-water levels have dropped from 200 ft (60 m) to more than 450 ft (135 m). The initial appearance of fissures is noted by: 1) small linear or en echelon hairline cracks, 2) irregularly spaced depressions, or 3) large, linear open holes. Negligible vertical offset and the separation of both sides suggest fissures are of tensile origin. Field evidence indicates subsidence fissures propagate upwards, only to be exposed after overlying sediments are eroded by intense rains or irrigation water (Figure 7).

Most fissures are less than a mile in length; however, one fissure near Picacho is 9.3 mi (15.8 km) long (Laney et al., 1978). Fissures generally are perpendicular to drainage, intercepting water that erodes the initial hair-line width cracks into gullies, as much as 15 ft (4.5 m) wide, and 10 ft (3 m) or more deep. Local lowering of base-level causes side-gullying, and the fissure frequently enlarges by subparallel or bifurcating cracks that cause large blocks to slump and fall into the main cavity. Because the fissures act as sinks, dense vegetative growth characteristically outlines the fissure trace.

Origin

Early ideas on the origin of fissures did not relate their occurrence to ground-water withdrawal, but to seismic events (Leonard, 1929) or to piping erosion (Fletcher et al., 1954). Several mechanisms related to ground-water withdrawal were subsequently proposed to explain the origin of earth fissures: localized differential compaction (Feth, 1951), hydrocompaction (Pashley, 1961), horizontal seepage forces (Lofgren, 1971), shrinkage of dewatered sediments (Holzer and Davis, 1976), and regional differential compaction (Bouwer, 1977). Recent work utilizing geophysical and geodetic surveying techniques support the hypothesis that many fissures are caused by differential subsidence localized by buried bedrock hills or fault scarps.

Turner (Feth, 1951) first speculated that an earth fissure in the Picacho Basin was located over the edge of a buried pediment. The association of steep gravity gradients with earth fissures there led some workers to suggest fissures may be located over buried fault scarps (Peterson, 1962; Schumann and Poland, 1969). Probably the first detailed geophysical investigation specifically of an earth fissure was suggested in 1971 for a fissure in east Mesa by Troy L. Péwé and Donal Ragan to W. A. Sauck of Arizona State University. Unpublished results from a gravity traverse confirmed the hypothesis that the fissure in east Mesa coincided with a buried bedrock ridge, as later reported by Anderson (1973). Subsequent studies have indicated that convex-upward gravity anomalies associated with many fissures arise from a similar buried bedrock profile (Sauck, 1975; Jennings, 1977; Christie, 1978; Pankratz et. al, 1979; and Jachens and Holzer, 1979). Precise geodetic leveling near the Picacho and Casa Grande Mountains indicates fissures do occur near points of maximum convex-upward curvature in subsidence profiles (Holzer and Pampeyan, 1981; Jachens and Holzer, 1982).

Description of Phoenix Fissure

A long crack in the ground was noted at a construction site near 40th Street and Lupine Avenue in northeast Phoenix (Figure 8) after heavy rains

←

Figure 6. Historical development of subsidence bowl, northeast Phoenix. A) Isolines in feet of land subsidence in northeast Phoenix, Arizona (1962–1970). B) Isolines in feet in land subsidence in northeast Phoenix, Arizona (1962–1974). C) Isolines in feet of land subsidence in northeast Phoenix, Arizona (1962–1977). D) Isolines in feet of land subsidence in northeast Phoenix, Arizona (1962–1982). 'F' indicates location of fissure.

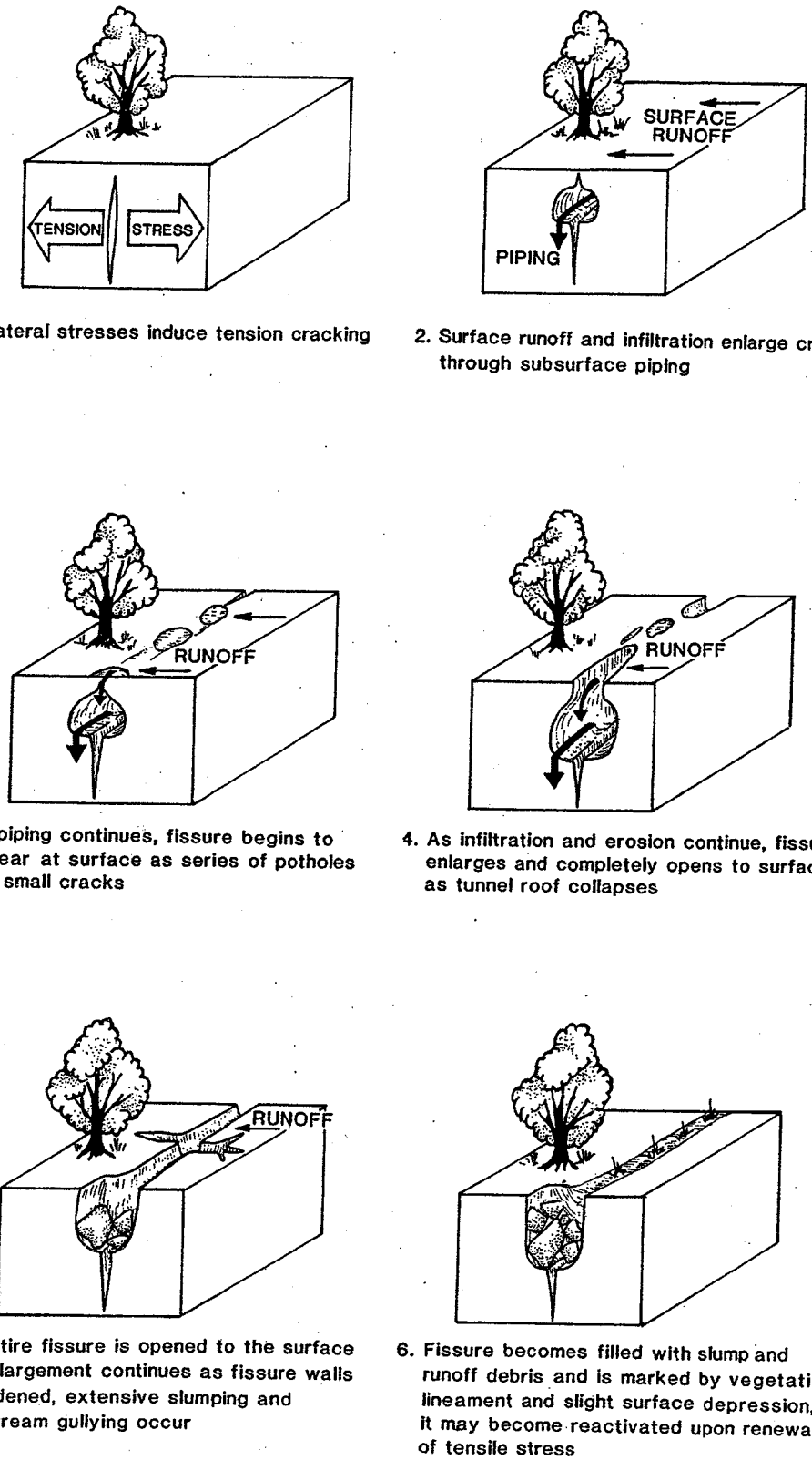

1. Lateral stresses induce tension cracking

2. Surface runoff and infiltration enlarge crack through subsurface piping

3. As piping continues, fissure begins to appear at surface as series of potholes and small cracks

4. As infiltration and erosion continue, fissure enlarges and completely opens to surface as tunnel roof collapses

5. The entire fissure is opened to the surface and enlargement continues as fissure walls are widened, extensive slumping and side-stream gullying occur

6. Fissure becomes filled with slump and runoff debris and is marked by vegetation lineament and slight surface depression, it may become reactivated upon renewal of tensile stress

Figure 7. Generalized states of fissure development (modified after Bell, 1981).

over the weekend of January 19, 1980. The fissure is the first known occurrence within the city of Phoenix.

Fissuring extended at least 400 ft (120 m) in an east–west direction, marked by hair-line cracks, small open holes, and a linear opening 15 ft (4.5 m) long, 8 ft (2.5 m) deep, and 15 in. (0.4 m) wide (Figure 8) (Péwé, 1980). Apparently part of the overlying soil cover was scraped off during construction activity, exposing the subterranean crack, and the collecting of rainwater in a retention basin eroded the large main cavity. No vertical offset was observed; the fissure appeared to be a typical example of a tensional ground failure (Péwé, 1980).

It was recommended that the fissure be back-filled with native soil to an elevation higher than the surrounding grade to create positive drainage away from the fissure, and a set-back zone was created along the fissure by rearrangement of lot lines for a greenbelt where no buildings were to be built (Péwé, 1980 pp. 10–11). The temporary halting of construction, modification of plans, hiring of consultants and other expenses incurred as a result of the fissure are estimated by the owners of the subdivision to have cost them approximately $500,000 (Thomas, 1982). Continued displacement along the fissure is indicated (1982) by 0.04 in. (1 mm) cracks that have become more numerous and lengthened in a newly constructed paved road across the original fissure trace, and in a concrete wall along 40th Street.

GRAVITY SURVEY

Gravity measurements were made at 311 stations, covering an area of approximately 11 mi^2 (28 km^2) in northeast Phoenix, during the summers of 1980 and 1981 (Figure 9). The LaCoste and Romberg model G gravimeter was used in the survey. A grid of 200 gravity stations was established at approximately 0.25 mi (0.4 km) increments (Larson and Péwé, 1981). The purpose of the grid arrangement was to determine the general trend and configuration of the subsurface bedrock topography. For purposes of this study, 'bedrock' means any consolidated rock that is essentially incompressible under effective stress changes caused by water-level decline. Bedrock includes all crystalline rock and indurated conglomerate.

The remainder of gravity stations were along detailed profiles across the earth fissure and potential fissure sites. Measurements were made along four detailed traverses run north–south perpendicular to the trend of the fissure near 40th Street and Lupine

Figure 8. Earth fissure in construction area at Lupine Avenue and 40th Street, Phoenix, Arizona. View is west across 40th Street. Fissure extends at least as far as the near sidewalk. (Photograph by Troy L. Péwé, No. 4484, January 27, 1980.)

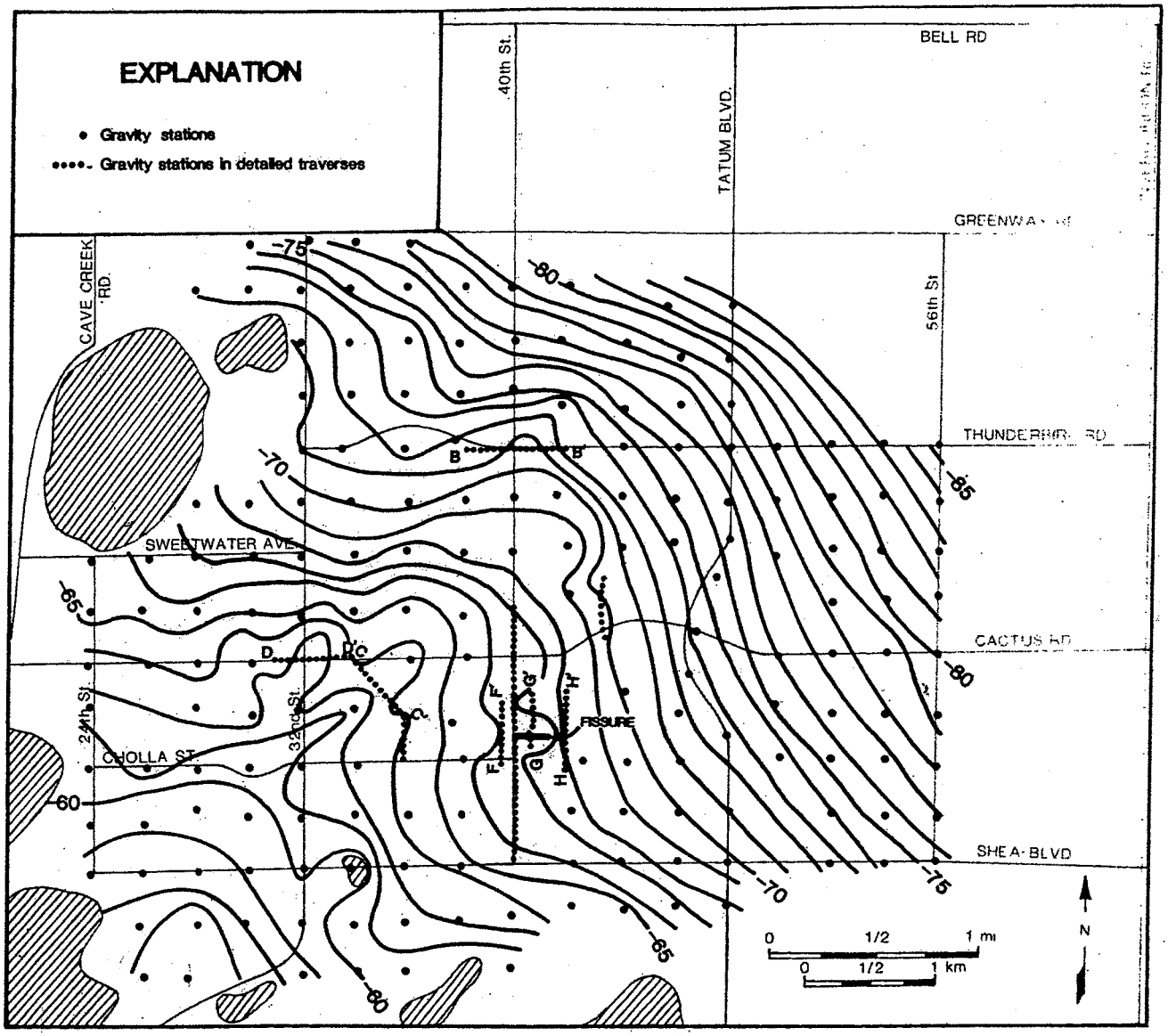

Figure 9. Complete Bouguer anomaly (mGal), northeast Phoenix, Arizona. (See Figures 12 and 14 for gravity profiles B-B', C-C', D-D', F-F', G-G', H-H'.)

Avenue. Stations were spaced 50 to 300 ft (15 to 90 m) apart across other gravity anomalies detected by the grid arrangement. From these profiles, the relief and maximum depth of the underlying anomalous masses could be estimated. All gravity measurements were tied to base stations within 1- to 3-hour closed loops.

Data Reduction

Gravity data was reduced to simple Bouguer anomalies with a program written by Campbell (1979) for use on a TI-59 (Texas Instrument) programmable calculator. Earth tide effects were partially removed in the drift correction. However, because earth tides do not vary linearly with time in contrast to the linear drift correction applied in the calculator program, there is a discrepancy between the drift-corrected and actual gravity values. From tidal variation recorded elsewhere (Nettleton, 1940; Telford et al., 1976), the maximum difference between observed and drift-corrected values in this survey during a 3-hour period (the maximum loop

closure time in this survey) is 0.03 mGal. Repeat measurements of the same gravity stations made less than 2 hours apart suggest a reading precision of 0.02 mGal for observed gravity during the survey.

Terrain corrections were calculated manually for zones B through J using the tables designed by Hammer (1939). Because many gravity readings were taken some distance away from the Phoenix Mountains, most terrain corrections were less than 0.10 mGal. A check for the accuracy of the terrain correction was made by two different orientations of the correction template for a gravity station with the maximum value near the southwestern corner of the survey. The difference in terrain correction values was 0.02 mGal; therefore, because the station value was slightly over 0.20 mGal, the uncertainty in terrain corrections is estimated at 10 percent of the total value. (Larson, 1982b).

Horizontal control for the survey was provided by both quarter-section maps (1:1,200) and 7.5-minute topographic maps (1:24,000). Latitudes were derived from these maps to the nearest 0.5 second according to the format of the reduction program, introducing an uncertainty of ±0.015 mGal.

Elevations were surveyed to within ±0.01 ft (.003 m) for 215 gravity stations by the Survey Section of the City of Phoenix Engineering Department. Surveyed stations were tied to benchmarks determined to be geodetically stable near bedrock outcrop (Sticht, 1981). The remaining station elevations were interpolated from 7.5-minute topographic maps with a 10-foot contour interval, and determined by Wild self-adjusting alidade. Thus, for 215 stations with elevations surveyed by the city of Phoenix, the maximum probable error in the Bouguer anomaly is ±0.4 mGal; for 26 stations surveyed with alidade at distances of 135 ft (40 m), it is ±0.05 mGal; for 14 stations surveyed with alidade at 0.25 mi (0.4 km) distances, it is ±0.07 mGal; and for the 56 stations where elevations were interpolated, it is ±0.12 mGal. Errors introduced by subsidence between the time of gravity station reading and later leveling had negligible effect on the total probable error, amounting to less than a 0.01 mGal increase in uncertainty.

Analysis and Interpretation

Results

Bouguer gravity values are highest near bedrock exposures in the southwest, and decrease to the northeast (Figure 9). Superposed on a salient where gravity contours are deflected towards the northeast near the center of the survey are several lesser gravity anomalies, including one associated with the fissure. Because the surface of the valley floor is smoothly sloping where gravity measurements were made, the gravity effect of topography is minimal; therefore, these small amplitude anomalies (generally less than 2 mGal) are assumed to arise from spatial changes in depth to bedrock. An anomaly of comparable size and amplitude associated with a small isolated bedrock outcrop on Shea Boulevard near the −61 mGal contour (Figure 9) tends to support this hypothesis. Although density variations within either the alluvium or bedrock could conceivably produce the observed anomalies, a similar study in the Picacho Basin by Jachens and Holzer (1979) suggests that in their gravity observations, such variations caused only minor gravity effects in most areas investigated. Relief on the interface between conglomerate and crystalline rock could also cause the observed gravity effects; however, a sufficient number of water-well records exist to resolve most of this ambiguity for the present study area.

Rock Densities

An average density of 2.70 g/cm^3 was calculated for 20 samples of igneous and metamorphic rocks in the adjacent Phoenix Mountains (Larson, 1982b). Dry bulk densities of 10 surface and two subsurface samples of indurated conglomerate averaged 2.30 g/cm^3. Because conglomerate constitutes approximately 10 percent of the Phoenix Mountains in the area surrounding the survey area, a weighted average density of 2.66 g/cm^3 was determined for consolidated rock in the Phoenix Mountains, and these values were also inferred for bedrock underlying alluvium. A reduction density of 2.67 g/cm^3 was used in all calculations.

In the survey area, unconsolidated basin fill is generally less than 1,000 ft (300 m) thick. No subsurface density measurements are known for Paradise Valley; however, average densities for the upper 1,000 ft (300 m) of alluvium in other similar basins of south-central Arizona range from 1.8 to 2.15 g/cm^3 (Davis, 1971; Eaton et al., 1972; West, 1972; Christie, 1978; and Hassamer and Dansareau, 1980). The density of alluvium was arbitrarily assigned a value of 2.0 g/cm^3; therefore, for two-dimensional gravity modelling a density contrast of 0.66 g/cm^3 was used. Subsurface conditions were also evaluated with standard formulas of simple geometric bodies (buried sphere and horizontal cylinders), and because observed anomalies could arise from relief on the

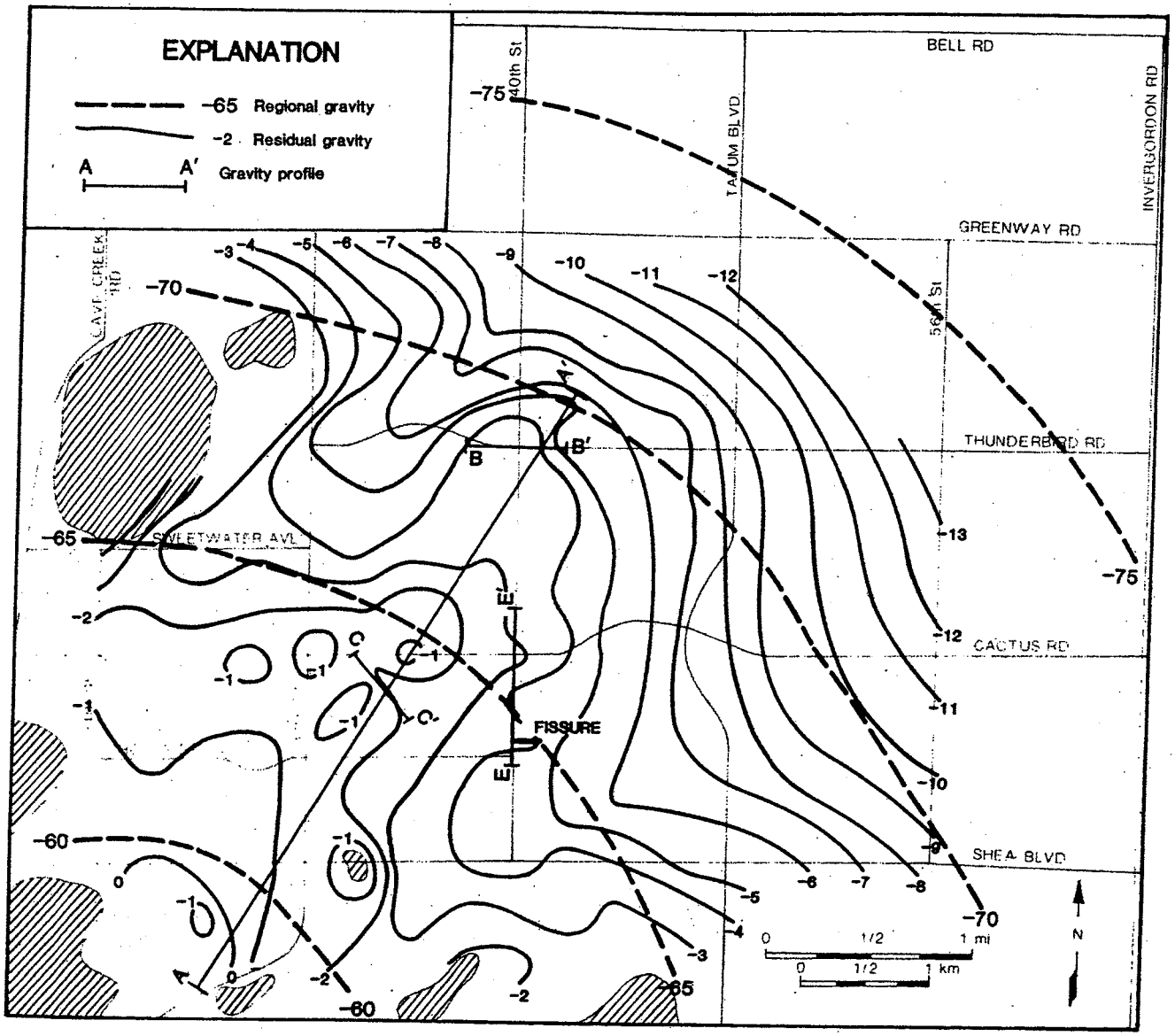

Figure 10. Regional and residual gravity (mGal), northeast Phoenix, Arizona. (See Figures 11, 13 for gravity profiles A-A', E-E'.)

interface between alluvium and either conglomerate or crystalline rock, a density contrast of 0.3 or 0.7 g/cm³ was used with this technique. Because alluvium densities are not precisely known, the uncertainty in density contrast chosen for depth estimates generally results in an estimated uncertainty of about ±75 (23 m) (Larson, 1982b). Although there are density differences between dry and saturated alluvium, all gravity models assumed "dry" alluvium to avoid analysis of a much more complex three-layer case.

Interpretation

Previous gravity surveys (Peterson, 1968; West and Sumner, 1973; and Lausten, 1974) over a larger area surrounding Paradise Valley indicate regional gravity decreases from the southwest to northeast at about 2.5 to 3.5 mGal per mile (1.5 to 2.1 mGal

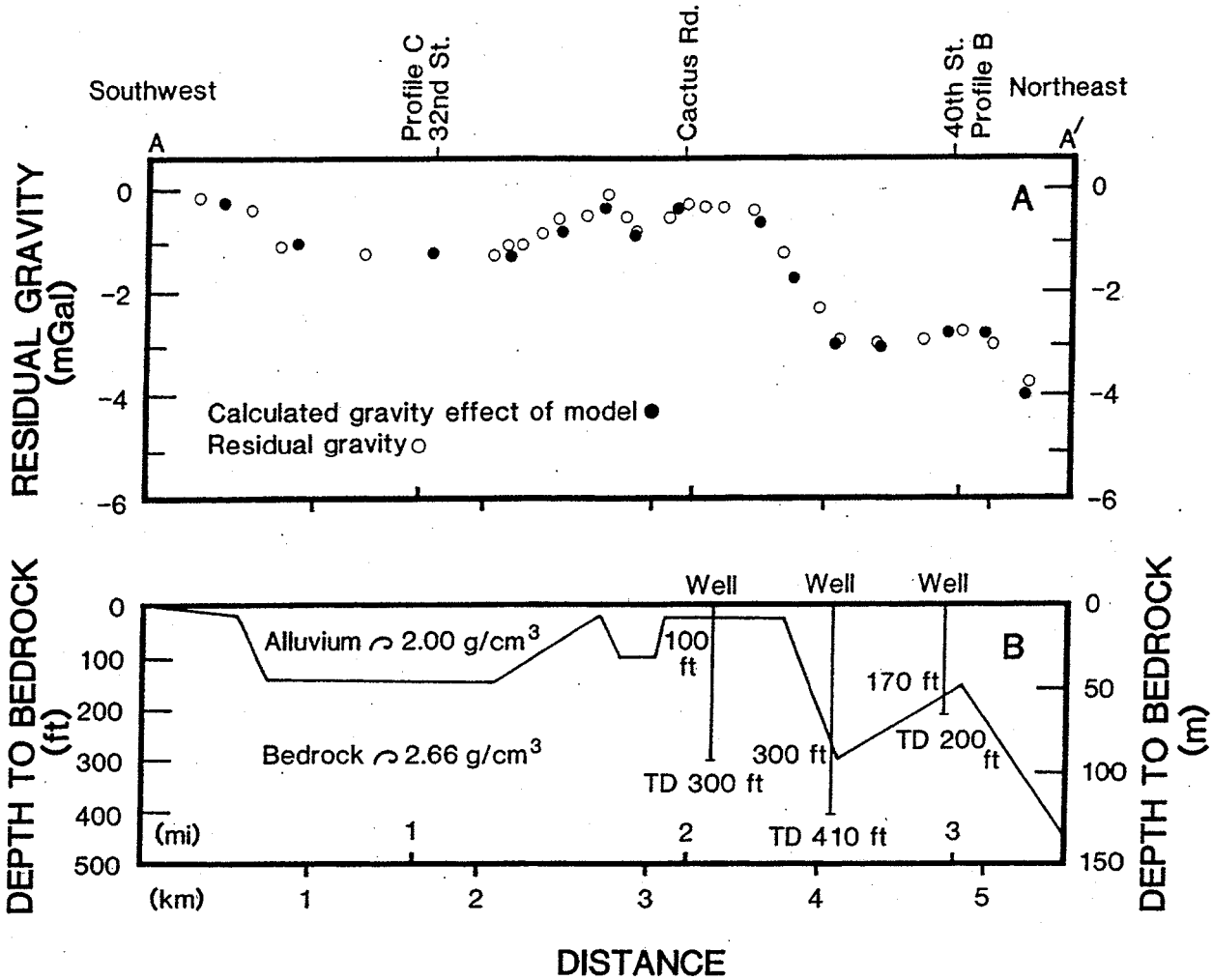

Figure 11. Two-dimensional gravity model of depth to bedrock, profile A-A′, northeast Phoenix, Arizona (see Figure 10 for location). A) Residual gravity and calculated gravity effect of model. B) Depth to bedrock model. Upper distance refers to depth where bedrock penetrated; lower distance (TD) is total depth of well. Vertical exaggeration = 6.6×.

per km) as a result of crustal thickening to the northeast under the Colorado Plateau. On the basis of this regional gravity gradient, and the trend of isogals in this survey, a curvilinear approximation of regional gravity was derived for the area (Figure 10). To obtain the residual gravity for evaluation of the buried bedrock surface, the regional is then subtracted from the complete Bouguer anomaly. This method mostly removes the gravity effect of crustal thickening to the northeast while the effects of large Basin-and-Range faults and buried bedrock relief remain.

Theoretically, the zero residual contour should approximate the alluvium-bedrock contact on the surface; however, residuals are also affected by density variations within the alluvium or bedrock, as well as large structural features. Gravity measurements in the survey area are significantly affected by a major NW–SE normal fault, with a minimum of 4,000 ft (1,200 m) of vertical displacement on the buried bedrock surface (Lausten, 1974) within 2 mi (3 km) of the eastern boundary of the gravity survey area.

The most prominent feature of the residual map

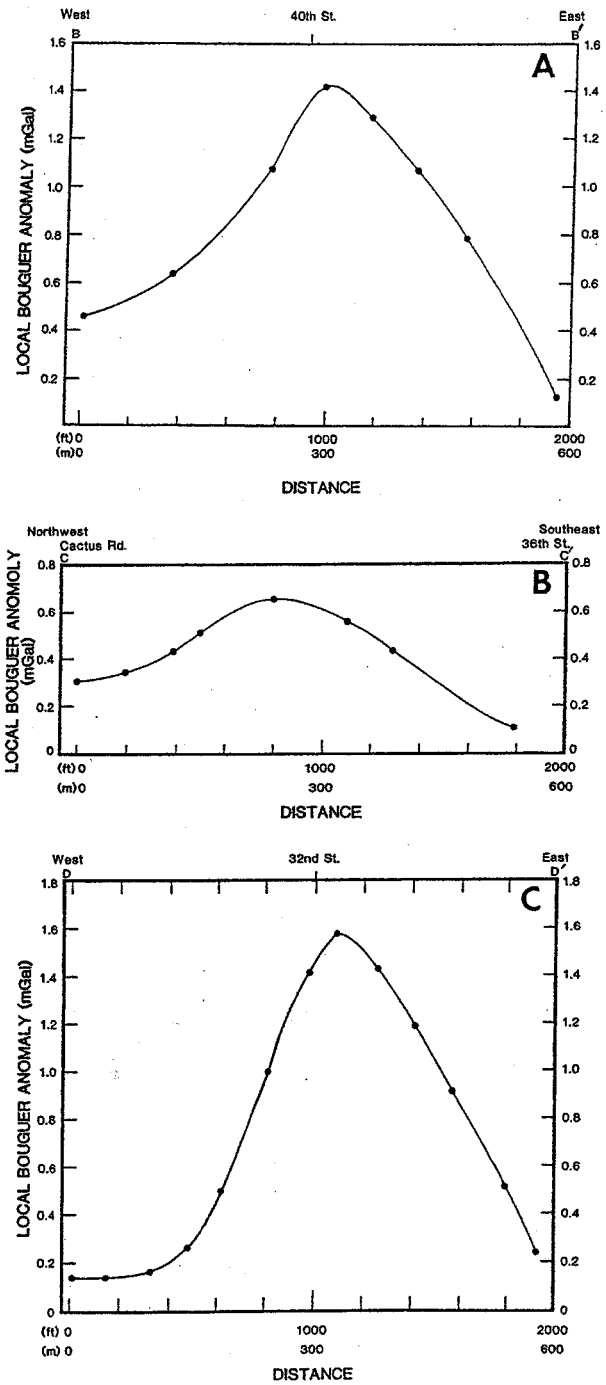

Figure 12. Gravity profiles B-B′, C-C′, D-D′. A) Gravity profile B-B′, Thunderbird Road (see Figure 9 for location). B) Gravity profile C-C′, Cactus Road to 36th Street (see Figure 9 for location). C) Gravity profile D-D′, Cactus Road (see Figure 9 for location).

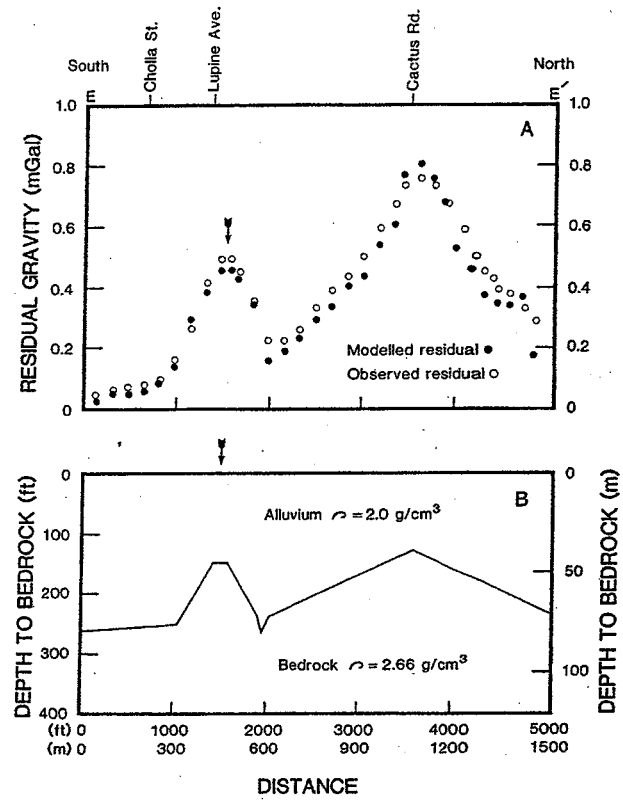

Figure 13. Two-dimensional gravity model of depth to bedrock, profile E-E′, 40th Street, northeast Phoenix, Arizona (see Figure 10 for location). Arrows indicate location of fissure. A) Residual gravity and calculated gravity effect of model. B) Depth to bedrock model. Vertical exaggeration = 6.6×.

is the large salient near the center of the survey area where residual contours are deflected toward the northeast (Figure 10). This area is interpreted to represent a shallow buried pediment area, with generally less than 500 ft (150 m) of alluvial cover. Crenulations and closures of residual highs trending southwest to northeast on the salient are interpreted to arise from topographic irregularities on the buried pediment, including the anomaly associated with the fissure. The salient could possibly be bounded on the northwest and southeast by downdropped fault blocks displaced by two NE–SW normal faults. The regular decrease of residuals towards the north and northeast is believed to arise from both a normal fault towards the northeast and an outer deeper part of the pediment gently sloping northeastward from a depth of 500 to 1,000 ft (150 to 300 m).

A profile of the buried bedrock surface (Figure 11B) along a southwest to northeast direction (profile A-A′) was modelled by fitting calculated resid-

uals to closely match observed values from the residual gravity map (Figure 10), using a program written by Haines and Campbell (1978) to calculate the gravity effect of two-dimensional Talwani-type prisms on a TI-59 calculator. The profile is perpendicular to the regional gravity trend. Buried bedrock hills along this profile (Figure 11) are interpreted to lie within 170 ft (50 m) of the surface, with as much as 250 ft (75 m) of relief.

Such an interpretation is supported by wells drilled in the area that indicate the buried bedrock surface slopes away from these inferred buried topographic highs. The wells drilled along profile A-A′ (Figure 11) yielded little or no water from these areas where a shallow depth to bedrock is interpreted. Because profile A-A′ does not perfectly intersect the maximum values along profiles B-B′ and C-C′ (Figures 10, 11) the depths to the tops of these buried features are probably slightly overestimated. On the basis of geometric models, the buried hills along profile B-B′ and C-C′ (Figure 11) are interpreted to be at depths from the surface of less than 170 ft (52 m) and 300 ft (90 m) respectively (Larson, 1982b, Appendix F, p. 139). Similar calculations for profile D-D′ (Figure 12C) suggest a bedrock hill is within 150 ft (45 m) of the surface near Cactus Road and 32nd Street.

Phoenix Fissure Site

The earth fissure near 40th Street and Lupine Avenue is spatially associated with the maxima of a 0.5 mGal convex-upward gravity anomaly (Figure 13A). Along profile E-E′, the width of the gravity anomaly [about 0.25 mi (0.4 km)] is an upper limit of the width of the buried hill; the anomaly half-width of about 360 ft (110 m) implies a maximum depth of 470 ft (145 m) for its source. Using the Haines and Campbell (1978) program of gravity modelling, the depth to the top of the buried knoll was calculated to be 150 ft (45 m) (Figure 13B), with at least 100 ft (30 m) of relief in a north–south direction. This interpretation appears appropriate since topographic features of similar areal extent in the Phoenix Mountains have total relief of 75 to 150 ft (22 to 45 m). Additional evidence for a shallow depth to bedrock near the fissure is a water well drilled 0.5 mi (0.8 km) NNE of the fissure (Figure 3), where indurated conglomerate was penetrated at a depth of 400 ft (120 m) before ending in crystalline rock at 735 ft (220 m). Along gravity profile H-H′ 650 ft (195 m) east of the fissure trace (Figure 14C), there is only subtle indication of a 'gravity ridge'; however, a convex-upward anomaly along profile F-F′ 500 ft (150 m) west of the fissure (Figure 14A) suggests the buried knoll that is inferred to underlie the fissure may extend some distance west of 40th Street.

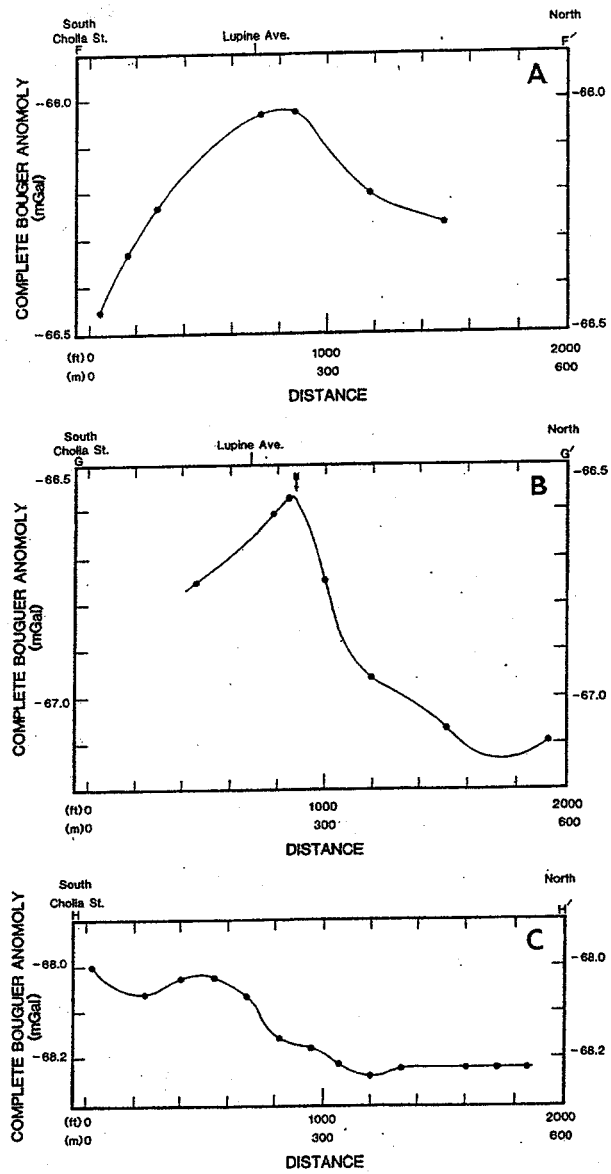

Figure 14. Gravity profiles F-F′, G-G′, H-H′ in northeast Phoenix, Arizona (see Figure 9 for location). A) Gravity profile F-F′. B) Gravity profile G-G′. Arrow indicates location of fissure. C) Gravity profile H-H′.

GEOLOGIC INTERPRETATION

General

Interpretation of well-drilling records, residual gravity maps, and gravity modelling provided the

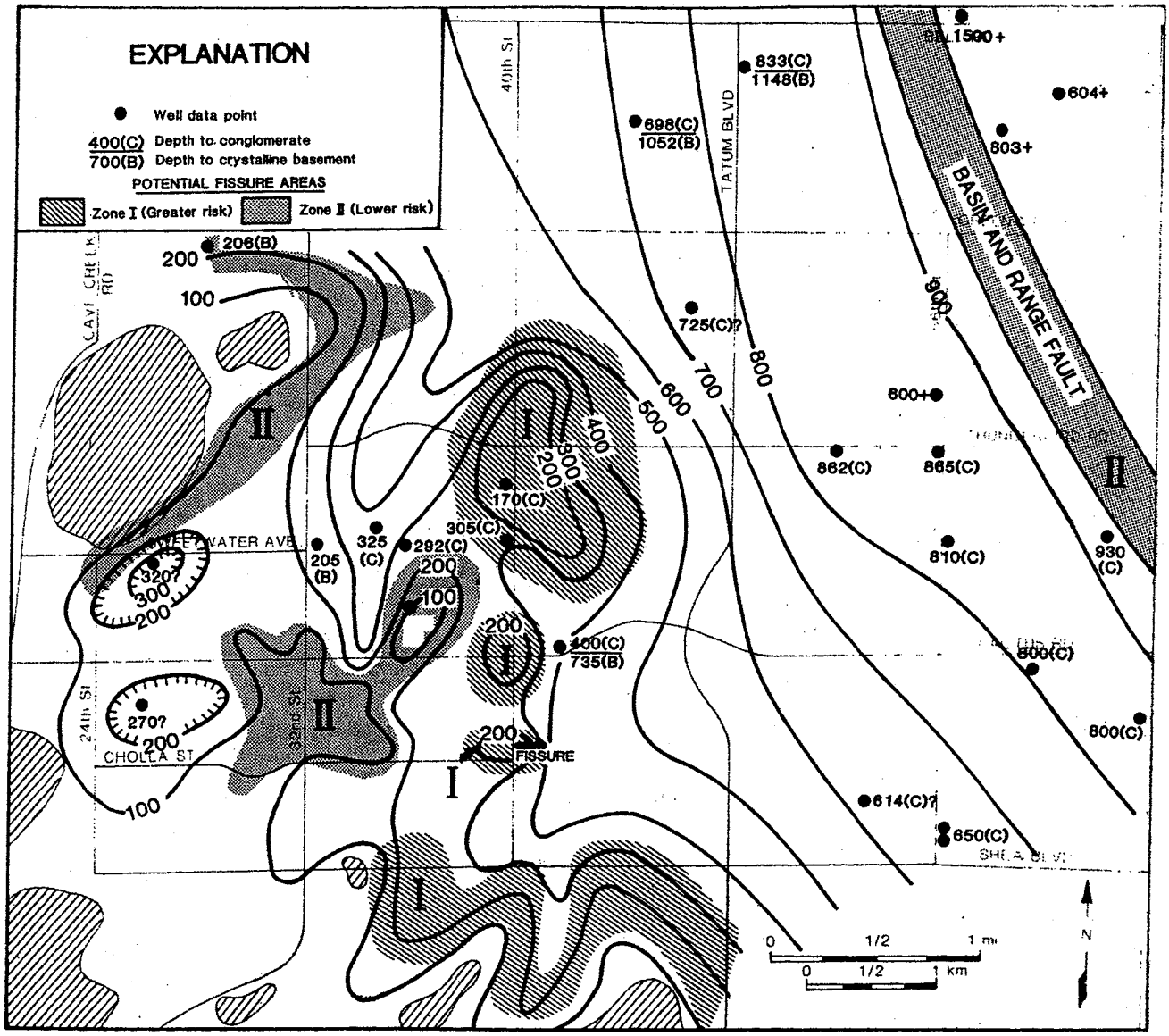

Figure 15. Estimated depth to bedrock in feet, and potential fissure areas, northeast Phoenix, Arizona. (Depth contours and boundaries of potential fissure areas are approximate as per limitations cited in the text. Data presented here is on a broad scale and does not preclude the necessity of specific site investigations.) Queried wells indicate inadequate information to determine depth to bedrock.

basis for the construction of a depth-to-bedrock map at a 100 ft (30 m) contour interval (Figure 15). The residual gravity map (Figure 10) suggests the direction of slope and relative location of topographic features on the buried bedrock surface; wells and detailed traverses provide control points for depth to bedrock in specific areas. Although the dimensions of gravity anomalies set limits on the width

and depth of the feature producing them, there is no unique solution that yields the exact dimensions. Because of inherent ambiguities in interpretation of gravity and well-drilling data, the map does not give absolute depth values but rather generalized values of both depth and relief of the buried bedrock surface.

On the basis of the resultant depth-to-bedrock map, a geologic interpretation of the subsurface topography and relation to subsidence and fissuring is possible. A large, inner-pediment, buried area at a shallow depth less than 500 ft (150 m) extends at least 2.5 mi (4.0 km) northeast from the Phoenix Mountains into Paradise Valley, (Larson and Péwé, 1982), with a series of hills and ridges with relief of 100 to 300 ft (30 to 90 m) (Figure 15). The buried bedrock features apparently follow the same northeast direction as the foliation and topographic expression common in the adjacent Phoenix Mountains. The Papago Park pediment about 3 mi (4 km) SE of the Phoenix Mountains probably is of comparable topographic and geologic complexity (Bales et al., 1980).

Bordering the inner pediment area to the north and northeast is an outer more deeply buried pediment of low relief; it slopes gently northeastward from a depth of approximately 500 ft (110 m) to 1,000 ft (300 m) (Figure 15). On the basis of well records and a steep gravity gradient to the north and east, a major NW–SE Basin-and-Range normal fault is interpreted to lie toward the center of the basin separating the pediment from thick unconsolidated deposits (Figure 15).

Subsurface geologic conditions control the spatial distribution of water levels and ground subsidence. Maximum depression of water levels has occurred on the deeper outer pediment accompanied by rapid subsidence. Wells on the more shallow parts of buried inner pediment yield little or no water (Figures 3, 10), and in these areas of high gravity values (Figure 8), negligible subsidence has been documented (Figure 6D). Subsidence increases wherever there are small local or broad regional increases in alluvial thickness; and the center of the subsidence bowl is near the center of the southern cone of depression of water level.

Origin of Phoenix Fissure

The fissure at 40th Street and Lupine Avenue was apparently localized by a small knoll on the shallow buried inner pediment (Figure 15) where differential compaction induced by dewatering of sediments across the buried knoll was sufficient to cause ground failure. The inferred buried hill associated with the fissure is on-line with a series of small bedrock hills that protrude above alluvium discontinuously in a southwest to northeast direction (Figure 15). Gravity results imply the buried irregularity underlies the fissure about 150 ft (45 m) at a depth comparable to the original water level in the area (Figure 16C). At this depth, differential compaction and the resultant horizontal strains generated are presumably much greater than if the feature were more deeply buried.

Differential subsidence since fissuring occurred has been measured over a one-year period (April, 1981 to April, 1982) by releveling the closely-spaced gravity stations along 40th Street (Figure 16B). As much as 0.17 ft (0.05 m) of subsidence occurred just north of Shea Boulevard and less than that elsewhere during this one-year interval. Near the fissure at Lupine Avenue, the ground surface apparently rose a minor amount. The striking similarity between subsidence curves and interpreted depth-to-bedrock profiles along 40th Street supports the argument that fissuring is associated with the crests of buried hills, where subsidence is at a local minimum. The small apparent rise of ground level near the crest of the buried hill may be a consequence of expansive soils (due to increased moisture content) or a 'buckling' effect of the 'slab' of alluvium as it bends over the buried hill. Another possibility is that the apparent rise is a result of small accumulated surveying errors, or releveling not being taken at the precise same spot of the gravity station.

Stress-Strain Relationship at Time of Fissuring

The differential compaction mechanism proposed to explain horizontal strain and tensile failure has been documented in both laboratory and analytical investigations by Lee and Shen (1969). Differential settlement causes differential horizontal displacements, resulting in tensile horizontal strain where subsidence profiles are convex-upward; and compressive strain where profiles are concave-upward. Horizontal strain attains maximum values at points of maximum curvature of the subsidence profile.

During the 12-month measuring period (April, 1981 to April, 1982) a maximum tensile strain of 0.013 percent was calculated at the fissure on 40th Street, and the accumulated tensile strain at the time of fissuring was calculated as 0.058 percent (Figure 16A), using the empirical formula described by Lee and Shen (1969). These results fall within the range

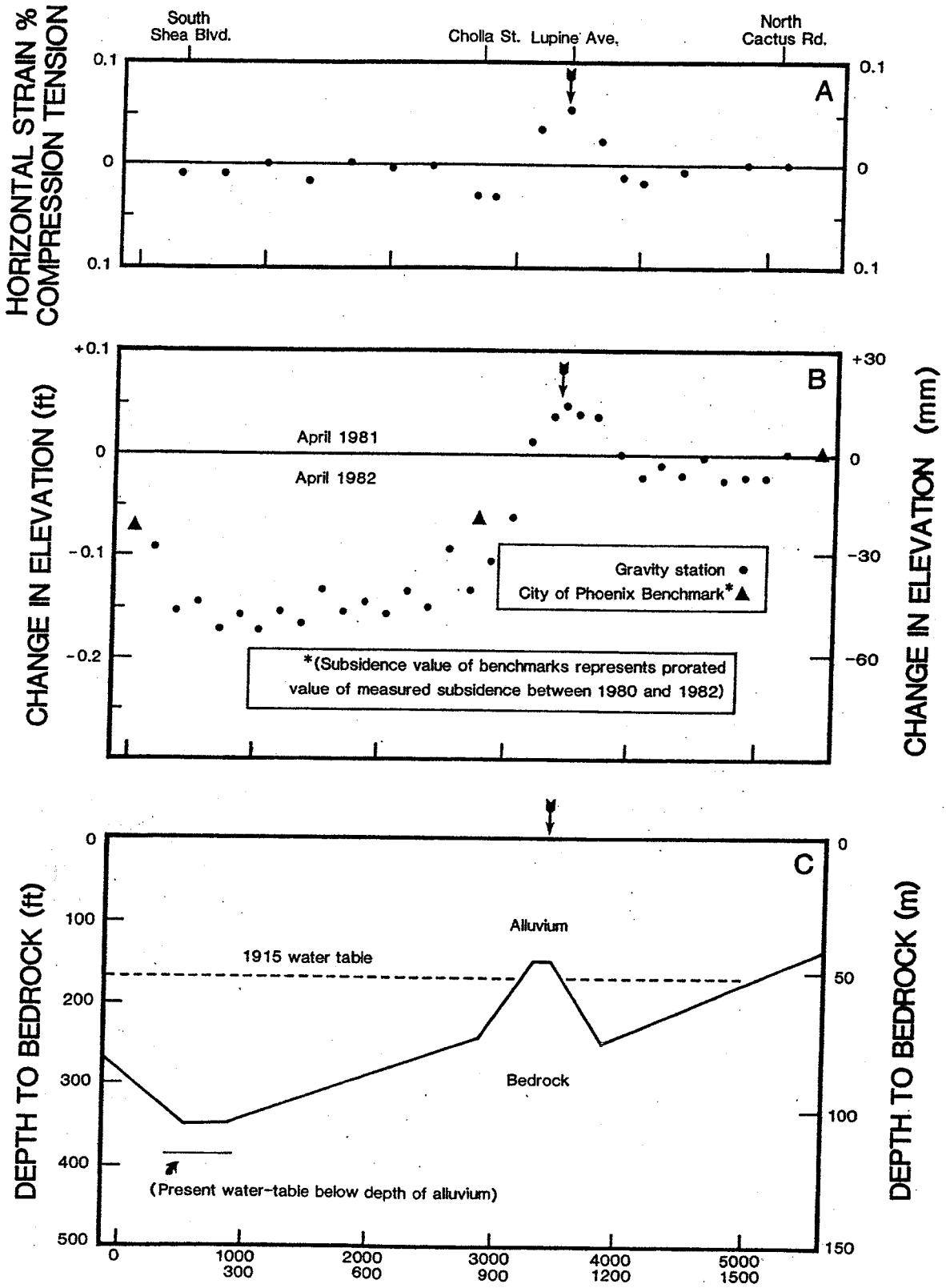
HORIZONTAL STRAIN %
COMPRESSION TENSION
South Shea Blvd.
Cholla St.
Lupine Ave.
North Cactus Rd.
A
B
April 1981
April 1982
Gravity station
City of Phoenix Benchmark*
*(Subsidence value of benchmarks represents prorated value of measured subsidence between 1980 and 1982)
CHANGE IN ELEVATION (ft)
CHANGE IN ELEVATION (mm)
C
Alluvium
1915 water table
Bedrock
(Present water-table below depth of alluvium)
DEPTH TO BEDROCK (ft)
DEPTH TO BEDROCK (m)

of measured and modelled tensile strain values in similar studies (Holzer and Pampeyan, 1981; Jachens and Holzer, 1982). In these studies, tensile strain at failure ranged from 0.02 to 0.07 percent, with average annual strains of 0.01 to 0.03 percent. Laboratory studies cited by Jachens and Holzer (1982) indicate that failure at less than 1 percent strain is common for relatively dry soils, such as those that occur in the study area.

Another technique, the finite-element method, was used by Ragan (Appendix A) to calculate both the vertical and horizontal stress/strain distribution near the fissure. The alluvium was treated as a homogenous isotropic elastic beam supported rigidly by the underlying bedrock. Results indicate that the maximum stress is nearly horizontal near the surface about 100 ft (30 m) south of the inferred crest of the buried hill. The zone of tensile stress is within 50 ft (15 m) of the surface, and is about 450 ft (135 m) wide along the profile.

Bouwer (1977) suggested another technique to calculate horizontal movements caused by land subsidence. A rigid slab of incompressible sediments is assumed to overlie deeper, more compressible fine-grained sediments. The rigid slab pivots across buried fault scarps or hills, undergoing a slight rotational movement. Trigonometric calculations for a rotating slab using the subsidence data along 40th Street yield an initial uneroded fissure width of about 0.5 in. (1.3 cm). This is in close agreement with observations of the initial width of the fissure.

CONCLUSIONS

The history of fissured basins in southern Arizona bears ample evidence that the initial fissure is later followed by complex patterns of multiple fissuring. Calculated horizontal strain and measured differential subsidence (Figure 15) at 40th Street and Lupine Avenue strongly suggest a potential for reactivation of the fissure at some future time. On the basis of the detailed gravity traverses (Figure 14), a future westward extension of the fissure is probable, with less than 600 ft (180 m) of eastward extension possible. Some time in the unknown future, because the local unconsolidated alluvium has been essentially dewatered near 40th Street and Lupine Avenue, residual compaction will cease, and therefore, fissuring and horizontal displacement should also cease.

In similar geophysical studies near fissures in southern Arizona (Anderson, 1973; Jennings, 1977; Pankratz et al., 1979; and Jachens and Holzer, 1979), it has been noted that several subparallel fissures frequently are a short distance away from the top of the inferred buried hills. Therefore, several subparallel fissures could possibly form in the immediate vicinity of 40th Street and Lupine Avenue.

Because differential subsidence over a buried bedrock knoll is the most plausible hypothesis for the origin of the fissure in northeast Phoenix, nearby similar buried topography detected by gravity measurements may be sites of future fissuring (Figure 17A). For example, the buried hill 0.6 mi (1.0 km) north of the fissure suggests that fissuring may occur in the future near 40th Street and Cactus Road (Figure 13).

Another geological setting of potential fissuring is near the "hinge-line" of subsidence; that is, the inferred boundary between subsiding and "stable" areas (Figure 17B) such as near Shea Boulevard peripheral to the mountains east of 32nd Street (Figure 15). This zone is dependent on a critical depth to bedrock related to the original ground-water level prior to pumping, a depth here of approximately 150 to 250 ft (45 to 75 m). Little or no compaction, and hence land subsidence, should occur where the thickness of the alluvial cover is less than the original depth to ground water, and for greater depths there is an increasing amount of subsidence. Fissures have been noted in such areas, presumably where tension attains local maximum values. A comparison between Figures 6D and 15 indicates the 'zero' or 'hinge-line' of subsidence in northeast Phoenix is largely controlled by depth to bedrock.

Some investigators have discussed structural as well as bedrock control of fissuring (Jennings, 1977; Holzer et al., 1979). Vertical offsets on surface fissures may result from differential compaction over buried fault scarps (Figure 17C). Differential subsidence and fissuring is possible across an inferred buried Basin-and-Range fault scarp in the eastern part of the study area (Figure 15); however, unlike

←

Figure 16. Computed horizontal surface strain (1980) at time of fissuring, land subsidence (April 1981 to April 1982), and interpreted depth to bedrock, 40th Street, northeast Phoenix, Arizona. Arrows indicate location of fissure. A) Horizontal surface strain; B) Land subsidence; C) Depth to bedrock. Based on two-dimensional gravity modelling (Figure 13) and depth-to-bedrock map (Figure 15). Vertical exaggeration = 6.6×.

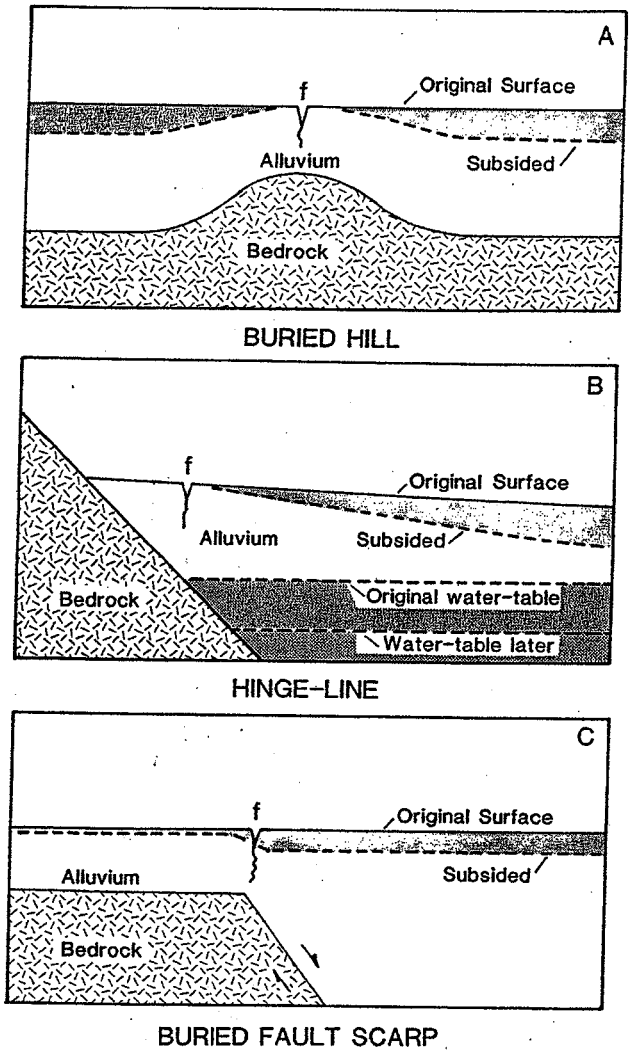

Figure 17. Diagrammatic sketch of geologic settings of areas of potential fissuring. A) Buried hill; B) Hinge-line; C) Buried fault-scarp.

the studies previously mentioned, most subsidence probably has occurred on the upthrown rather than the downthrown fault block in northeast Phoenix (Figures 6D, 15); so therefore, at the present, fissuring seems unlikely in this area. In addition, small faults bordering the inner pediment could localize fissuring.

Potential fissure areas are divided into two zones of susceptibility on the basis of evaluating all available subsidence and subsurface data (Figure 15). All potential fissure areas are generalized according to the limitations of the depth to bedrock interpretation. Zone I (greater risk) is the most critical—a steep subsidence gradient (Figure 6D) and the interpreted subsurface bedrock configuration suggest that fissuring in these areas is highly probable. Areas in Zone II (lesser risk) are in a geologic environment conducive to fissuring, but because significant land subsidence has not been recorded in these areas thus far, fissuring is not likely to occur until the subsidence bowl expands and deepens. Fissuring caused by mechanisms other than differential compaction (horizontal seepage stress, desiccation, hydrocompaction, swelling clay) are not considered in this study.

The growth of the subsidence bowl (Figure 6) suggests that it will expand farther, particularly toward the north and east; subsidence has been measured to the east in the city of Scottsdale. The extent of land subsidence to the south into the town of Paradise Valley, however, is not known.

The apparent lack of significant subsidence near the northern cone of depression of water levels (Figures 3, 6) may be because the draining of a 200-foot (60 m) thick clay layer is slow, and therefore, compaction up until now has been negligible. However, because static water levels are nearing the base of the clay unit, compaction presumably will be accelerated when the clay unit can be drained both from above and below instead of presently only from above. Greater subsidence in this area may possibly cause fissuring north of Cactus Road and west of 40th Street. There is insufficient data on compaction and material properties of the subsurface to fully evaluate the potential of future land subsidence in northeast Phoenix; however, given known thicknesses of alluvium and present subsidence rates near the center of the subsidence bowl, more than 9 ft (3 m) of land subsidence is possible if this area were completely dewatered.

Cooperation of city, state, and federal governments and education of the public is essential to adequately resolve problems associated with earth fissuring and land subsidence. Avoiding costly damage may require modification and replacement of existing engineering structures, and rezoning similar to ordinances enacted in other communities in the U.S., that govern land use in areas that are flood-prone or near active faults. Of course, without the long-term solution of conservation and appropriate use of limited ground-water resources, temporary 'fixes' are destined to fail. Prediction of earth fissuring and subsidence, therefore, may prove particularly useful during this period of overdraft of ground water.

ACKNOWLEDGEMENTS

Appreciation is extended to James Attebery, City Engineer, and David Harmon, Assistant City Engineer, for cooperation and encouragement in this study, and for recommending partial funding. City officials that provided valuable land survey and water well data, and laboratory testing included Raymond Freise, Brian Sticht, Ken Daly, Ralph Moska, Ellwood Orth, Ray Acuna, and Russ Schnormeier. Special thanks to David Campbell and Robert Jachens, Geophysicists, U.S. Geological Survey and Robert West, Geophysicist, Mining Geophysical Surveys for assistance, and their in-depth reviews, particularly regarding the geophysical part of the study. Reviews by Donal Ragan, Department of Geology, Arizona State University and Herman Bouwer, U.S. Department of Agriculture Water Conservation Laboratory were most helpful.

The sharing of information from similar research by Herb Schumann, Robert Laney, Richard Raymond, John Sumner, Carl Winikka, and Ed Nemecek was most helpful. Ron Vittorini assisted with important field work. Elaine McGovern and Alice Spears typed preliminary and final copies of the paper. We also would like to thank Sue Selkirk and Greg Sager for drafting of figures.

REFERENCES

ANDERSON, S. L., 1973, *Investigation of the Mesa Earth Crack, Arizona, Attributed to Differential Subsidence Due to Ground Water Withdrawal:* Unpublished Master's Thesis, Arizona State University, Tempe, AZ, 111 p.

ARIZONA DEPARTMENT OF TRANSPORTATION, 1981, *1981 NGS Level Line, Apache Junction to I-10 at Miller Road, ADOT Preliminary Adjustment,* Unpublished Report: Arizona Department of Transportation, Highways Division, Photogrammetry and Mapping Services, Phoenix, AZ, 192 p.

ARTEAGA, F. E.; WHITE, N. D.; COOLEY, M. E.; AND SUTHEIMER, A. F., 1968, *Ground Water in Paradise Valley, Maricopa County, Arizona,* Arizona State Land Department, Water-Resources Report 35: Arizona State Land Department, Phoenix, AZ, 767 p.

BALES, J. T.; SCHULTEN, C. S.; AND PÉWÉ, T. L., 1980, *Environmental Geology of the Tempe Quadrangle, Maricopa County, Arizona,* Unpublished Report: City of Tempe, Tempe, AZ, 16 maps, scale 1:24,000.

BELL, J. W., 1981, *Subsidence in Las Vegas Valley,* Nevada Bureau of Mines and Geology Bulletin 95: Mackay School of Mines, University of Nevada, Reno, NV, 84 p.

BOUWER, HERMAN, 1977, Land subsidence and cracking due to ground water depletion: *Ground Water,* Vol. 15, No. 5, pp. 358–364.

CAMPBELL, D. L., 1979, *Texas Instruments Model 59 Hand-Calculator Program to Reduce Gravity Data to Simple Bouguer Anomaly,* Unpublished Report: U.S. Geological Survey, Denver, CO, 7 p.

CHRISTENSON, G. E. AND PÉWÉ, T. L., 1978, *Environmental Geology of the McDowell Mountains, Maricopa County, Arizona,* Arizona Bureau of Geology and Mineral Technology Geologic Investigation Series Map GI-1-A-B: Arizona Bureau of Geology and Mineral Technology, Tucson, AZ, scale 1:24,000.

CHRISTIE, F. J., 1978, *Analysis of Gravity Data From the Picacho Basin, Pinal County, Arizona:* Unpublished Master's Thesis, University of Arizona, Tucson, AZ, 105 p.

CORDY, G. E.; HOLWAY, J. V.; AND PÉWÉ, T. L., 1977, *Environmental Geology, Paradise Valley Quadrangle, Maricopa County, Arizona,* Unpublished Report: City of Scottsdale, Scottsdale, AZ, 14 maps, scale 1:24,000.

DALY, KEN, 1982, personal communication, Phoenix Water Production Office, Phoenix, AZ, 85018.

DAVIS, A. P., 1897, *Irrigation Near Phoenix, Arizona,* U.S. Geological Survey Water-Supply and Irrigation Paper No. 2: U.S. Geological Survey, Denver, CO, 95 p.

DAVIS, R. W., 1971, An analysis of gravity data from the Tucson basin, Arizona: *Arizona Geological Society Digest,* Vol. 9, pp. 103–121.

EATON, G. P.; PETERSON, D. L.; AND SCHUMANN, H. H., 1972, *Geophysical, Geohydrological and Geochemical Reconnaissance of the Luke Salt Body, Central Arizona,* U.S. Geological Survey Professional Paper 753: U.S. Geological Survey, Denver, CO, 28 p.

ELLIOTT, M. R., 1969, *Investigation of Vertical Displacement of Ground Surface, Phoenix-Mesa area, Arizona,* U.S. Geological Survey Unpublished Report: U.S. Geological Survey, Denver, CO., 80 p.

FETH, J. H., 1951, *Structural Reconnaissance of the Red Rock Quadrangle, Arizona,* U.S. Geological Survey Open-File Report: U.S. Geological Survey, Denver, CO, 32 p.

FLETCHER, J. E.; HARRIS, K.; PETERSON, H. B.; AND CHANDLER, V. N., 1954, Piping (a symposium): *EOS American Geophysical Union Transactions,* Vol. 35, pp. 258–262.

HAINES, D. N. AND CAMPBELL, D. L., 1978, *Texas Instruments Model 59 Hand-Calculator Program to Calculate Gravity Anomaly over 2-D Prisms of as Many as 22 Vertices,* U.S. Geological Survey Unpublished Report: U.S. Geological Survey, Denver, CO, 7 p.

HAMMER, S. I., 1939, Terrain corrections for gravimeter stations: *Geophysics,* Vol. 4, pp. 184–194.

HASSAMER, J. H. AND DANSAREAU, D. C., 1980, *Gravity Survey in Parts of Maricopa and Pinal Counties, Arizona,* U.S. Geological Survey Open-File Report 80-1255: U.S. Geological Survey, Denver, CO, 9 p.

HOLZER, T. L., 1981, Preconsolidated stress of aquifer systems in areas of induced land subsidence: *Water Resources Research,* Vol. 17, No. 3, pp. 693–704.

HOLZER, T. L. AND DAVIS, S. J., 1976, *Abstract,* Earth fissures associated with water-table declines: *Geological Society of America, Abstracts with Programs,* Vol. 8, No. 6, pp. 923–924.

HOLZER, T. L.; DAVIS, S. N.; AND LOFGREN, B. E., 1979, Faulting caused by ground-water extraction in southcentral Arizona: *Journal of Geophysical Research,* Vol. 84, No. B2, pp. 603–612.

HOLZER, T. L. AND PAMPEYAN, E. H., 1981, Earth fissures and localized differential subsidence: *Water Resources Research,* Vol. 17, No. 1, pp. 223–227.

JACHENS, R. C. AND HOLZER, T. L., 1979, Geophysical investigations of ground failure related to ground-water withdrawal, Picacho Basin, Arizona: *Ground Water,* Vol. 17, No. 6, pp. 574–585.

JACHENS, R. C. AND HOLZER, T. L., 1982, Differential compaction mechanism for earth fissures near Casa Grande, Arizona: *Geological Society of America Bulletin,* Vol. 93, pp. 998–1012.

JENNINGS, M. D., 1977, *Geophysical Investigations Near Subsidence Fissures in Northern Pinal and Southern Maricopa Counties, Arizona:* Unpublished Master's Thesis, Arizona State University, Tempe, AZ, 102 p.

LANEY, R. L.; RAYMOND, R. H.; AND WINIKKA, C. C., 1978, *Maps Showing Water Declines, Land Subsidence and Earth Fissures in South-Central Arizona,* U.S. Geological Survey Water Resources Investigations Open File Report 78–83: U.S. Geological Survey, Denver, CO, scale 1:250,000, 2 sheets.

LARSON, M. K., 1982a, *Prediction of Earth-Fissures Related to Ground-Water Withdrawal in the Greater Phoenix Area, Maricopa County, Arizona,* Unpublished Report: Arizona State University, Tempe, AZ, 16 p.

LARSON, M. K., 1982b, *Origin of Land Subsidence and Earth Fissures, Northeast Phoenix, Arizona:* Unpublished Master's Thesis, Arizona State University, Tempe, AZ, 151 p.

LARSON, M. K. AND PÉWÉ, T. L., 1981, Gravity methods applied to the investigation and prediction of earth fissures related to groundwater withdrawal in Phoenix, Arizona: *EOS, American Geophysical Union Transactions,* Vol. 62, No. 45, pp. 863.

LARSON, M. K. AND PÉWÉ, T. L., 1982, *Abstract,* Investigation and prediction of earth fissures related to ground-water withdrawal, Phoenix, Arizona: *Geological Society of America, Abstracts with Programs,* Cordilleran Section, Vol. 14, No. 4, p. 179.

LAUSTEN, C. D., 1974, *Gravity Methods Applied to the Geology and Hydrology of Paradise Valley, Maricopa County, Arizona:* Unpublished Master's Thesis, Arizona State University, Tempe, AZ, 137 p.

LEE, K. L. AND SHEN, C. K., 1969, Horizontal movements related to subsidence: *Journal of the Soil Mechanics and Foundations Division, American Society of Civil Engineers,* Vol. 95, pp. 139–166.

LEE, W. T., 1905, *Underground Waters of Salt River Valley, Arizona,* U.S. Geological Survey of Water-Supply Paper 136: U.S. Geological Survey, Denver, CO, 196 p.

LEONARD, R. J., 1929, An earth fissure in southern Arizona: *Journal of Geology,* Vol. 37, No. 8, pp. 765–774.

LOFGREN, B. E., 1971, Significant role of seepage stresses in compressible aquifer systems: *American Geophysical Union Transactions,* Vol. 52, No. 11, p. 832.

MARSDEN, L. E., 1960, How the national map accuracy standards were developed: *Surveying and Mapping,* Vol. 20, pp. 427–439.

MCDONALD, H. R.; WOLCOTT, H. N.; AND BLUHM, F. I., 1947, *Geology and Ground Water Resources of Paradise Valley, Maricopa County, Arizona: with a Section on Quality of Water, by J. D. Hem,* U.S. Geological Survey Open-File Report: U.S. Geological Survey, Denver, CO, 34 p.

MEINZER, O. E. AND ELLIS, A. J., 1915, *Ground Water in Paradise Valley, Arizona,* U.S. Geological Survey Water-Supply Paper 375-B: U.S. Geological Survey, Denver, CO, pp. 51–75.

NETTLETON, L. L., 1940, *Geophysical Prospecting for Oil:* McGraw-Hill, New York, NY, 442 p.

PANKRATZ, L. W.; HASSAMER, J. H.; AND ACKERMANN, H. D., 1979, Geophysical studies relating to earth fissures in central Arizona: *Geophysics,* Vol. 44, No. 3, p. 367.

PASHLEY, E. F., JR., 1961, Subsidence cracks in alluvium near Casa Grande, Arizona: *Arizona Geological Society Digest,* Vol. 4, pp. 95–101.

PETERSON, D. E., 1962, *Earth Fissuring in the Picacho Area, Pinal County, Arizona:* Unpublished Master's Thesis, University of Arizona, Tucson, AZ, 35 p.

PETERSON, D. L., 1968, *Bouguer Anomaly Map of Parts of Maricopa, Pima, Pinal, and Yuma Counties, Arizona,* U.S. Geological Survey Geophysical Investigations Map GP-615: U.S. Geological Survey, Denver, CO, scale 1:250,000.

PÉWÉ, T. L., 1980, *Earth Crack, 40th Street and Lupine, Phoenix, Arizona,* Unpublished Report: Tempe, AZ, 13 p.

PÉWÉ, T. L. AND LARSON, M. K., 1982, *Origin of Land Subsidence and Earth Fissures, Northeast Phoenix, Arizona:* City of Phoenix, Engineering Department, Phoenix, AZ, 151 p.

RAYMOND, RICHARD H., 1980, personal communication, Geologist, U.S. Bureau of Reclamation, Phoenix, AZ.

SAUCK, W. A., 1975, Geophysical studies near subsidence fissures in central Arizona: *EOS, American Geophysical Union Transactions,* Vol. 56, No. 12, pp. 984–985.

SCHUMANN, H. H., 1974, *Land Subsidence and Earth Fissures in Alluvial Deposits In the Phoenix Area, Arizona,* U.S. Geological Survey Miscellaneous Investigations Series Map I-845: U.S. Geological Survey, Denver, CO, scale 1:250,000.

SCHUMANN, H. H. AND POLAND, J. F., 1969, Land subsidence, earth fissures, and groundwater withdrawal in southcentral Arizona, U.S.A., In *Land Subsidence:* Tokyo International Association of Science Hydrology Publication 88, Vol. 1, pp. 295–302.

SHANK, P. C. AND PÉWÉ, T. L., 1973, *Environmental Geology in the Phoenix Mountains, Maricopa County, Arizona,* Unpublished Report: City of Phoenix, Phoenix, AZ, 8 maps, scale 1:15,000.

STICHT, BRIAN G., 1981, personal communication, Survey Engineer, City of Phoenix Engineering Department, Phoenix, AZ.

TELFORD, W. M.; GELDART, L. P.; SHERIFF, R. E.; AND KEYS, D. A., 1976, *Applied Geophysics:* Cambridge University Press, Cambridge, England, 860 p.

THOMAS, RICHARD A., 1982, personal communication, Senior Principal, Staman and Thomas Co., Phoenix, AZ.

U.S. DEPARTMENT OF THE INTERIOR, BUREAU OF RECLAMATION, 1976, Geology and ground-water resources report, Maricopa and Pinal counties, Arizona. In *Lower Colorado River Region* (a report for the Central Arizona Project), Phoenix, AZ, Vol. 1, 105 p.

WELSCH, D. G. AND PÉWÉ, T. L., 1979, *Environment Geology of the McDowell Mountains Area, Maricopa County, Arizona,* Geologic Investigation Series Map GI-1-G: Arizona Bureau of Geology and Mineral Technology, Tucson, AZ, scale 1:24,000.

WEST, R. E., 1972, *A Regional Bouguer Gravity Anomaly Map of Arizona:* Unpublished PhD Dissertation, University of Arizona, Tucson, AZ, 186 p.

WEST, R. E. AND SUMNER, J. S., 1973, *Bouguer Gravity Anomaly Map of Arizona:* Department of Geosciences, University of Arizona, Tucson, AZ, scale 1:1,000,000, 1 sheet.

WILSON, E. D.; MOORE, R. T.; AND PEIRCE, H. W., 1957, *Geo-*

logic Map of Maricopa County, Arizona: Arizona Bureau of Geology and Mineral Technology, Tucson, AZ, scale 1:375,000, 1 sheet.

WINIKKA, CARL C. AND WOLD, P. D., 1976, Land subsidence in central Arizona, In *Second International Symposium on Land Subsidence,* International Association of Hydrological Sciences Publication 121: Anaheim, CA, pp. 95–103.

APPENDIX A

Finite Element Model of the Phoenix Earthcrack

Donal M. Ragan
Department of Geology,
Arizona State University,
Tempe, AZ

INTRODUCTION

A necessary step toward an understanding of earth cracks is a consideration of the mechanical factors which are involved in their formation, and this is especially true if we wish to predict accurately the time and place of the cracking. The best way to do this is with the aid of a model.

Several attempts have already been made to model some aspects of the process. Lee and Shen (1969) considered the horizontal movements which accompany the subsidence of both artificial and natural sedimentary materials in a number of settings.

Bouwer (1977), in a study aimed specifically at the relation between cracks and ground-water depletion, modeled the subsidence alluvial basin by a simple slab. He considered two cases. The first involved the development of a crack above a buried scarp. The second, and the one of interest here, involved the bending of a slab over a buried hill. Although the results are both interesting and reasonable, they are still rather general.

With the subsurface data acquired by Larson and Péwé during this study, it is now appropriate to attempt to model the processes involved in the formation of an earth crack at a specific site.

THE MODEL

The analytical approach used is the finite element method, whereby a two-dimensional section through a deformable body is subdivided into a mesh of discrete elements, each of which is assumed to be in a homogeneous state of stress and strain. The solution of the problem, subject to appropriate boundary conditions, is then solved algebraically with the aid of a computer. Where it is anticipated that the state of stress changes rapidly larger numbers of small elements are used. Finite element programs are widely available; the one used in this study is from Desai and Abel (1972).

In order to model the Phoenix crack, a cross section was constructed from the results of the present study. Because the gravity method cannot resolve local details, the buried hill which seems to have localized the crack was assumed to be smooth and symmetrical, but with reasonable slopes and height (Figure 18A). The alluvial material overlying the hill as treated as an irregular beam of elastic material, supported rigidly by the bedrock surfaces in the vicinity of the hill. To the south, away from the hill, the lower surface of this beam was taken as a horizontal plane at a depth of 250 ft (76.2 m); the ground-water withdrawal has been mostly from below this depth. This surface was then displaced downward to simulate subsidence; the southern end of the beam was prevented from moving laterally. These vertical displacements, as well as those at the surface are shown in Figure 18A.

Lacking detailed knowledge of the properties of the actual material at depth, it was assumed to be completely described by a Young's modulus of 10^6 lb/ft^2 and Poisson's ratio of 0.3. These are reasonable values for alluvium composed of a mixture of sand and clay (Bouwer, 1977, p. 362).

With the mesh assumed to be in a state of plane strain, together with the boundary conditions and material properties, the displacement of each node and the stress within each element is then obtained. These displacements and stresses have two distinct causes. The first is due to the weight of the slab. The second is the result of the bending which accompanies the subsidence.

RESULTS

In order to facilitate comparison with the field measurements, only the surface displacements are shown graphically in Figure 18A. These depart only slightly from the specified displacements along the lower surface of the beam.

The magnitudes and orientations of the principal stresses in each element are shown in Figure 18B. Of special interest are the near-surface elements over the buried hill where tensile stresses occur, and these are specially marked. The principal tensile stresses vary only a degree or two from horizontal. The magnitudes of these stresses are also shown graphically, where it can be seen that the maximum tensile stress is about 2,430 psf (about 17 psi). This maximum is associated with the centroid of the element at a depth

Figure A Displacements

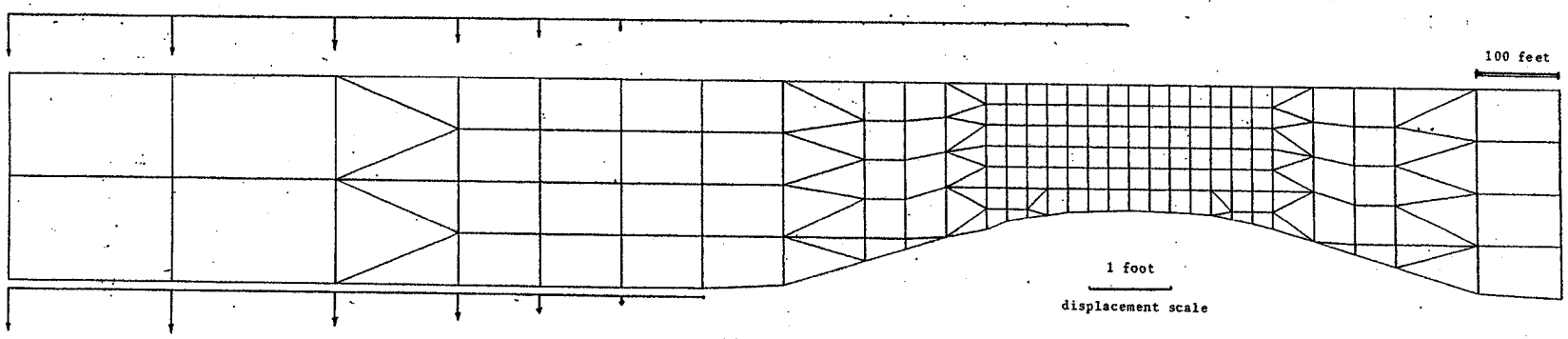

Figure B Stress distribution

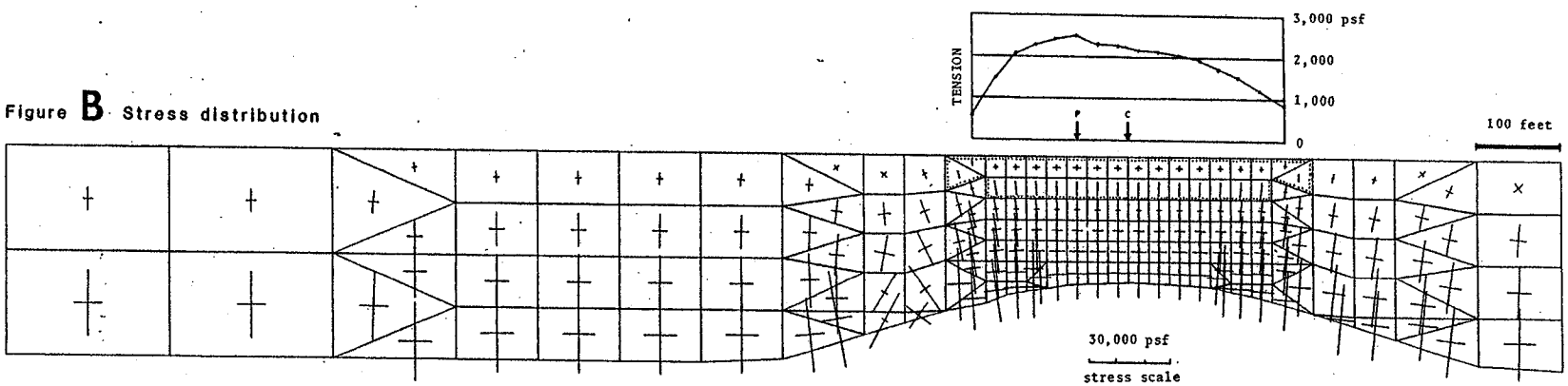

of 12.5 ft (3.8 m); linear extrapolation to the surface suggests that the maximum there would be about 3,400 psf (or about 24 psi). Such stresses are almost certainly in excess of the tensile strength of the slightly consolidated alluvial material, though it should be emphasized that these magnitudes depend on the chosen value of Young's modulus. The longitudinal strain at the surface of this same element is 0.19 percent based on surface displacement.

The point of maximum tension is also the predicted location of the earth crack, and it occurs 50–75 ft (15–23 m) to the south of the real crack. There are several possible explanations for this small discrepancy. The gravity method is not sensitive enough to precisely locate the hill crest; there may also be some topographic irregularity on the hill which influences the actual crack. In addition, because displacements were made in the model only on the south end, the fissure may have been offset from the ridge crest in this direction.

Finally, it should be noted that the stresses are tensile to a maximum depth of about 50 ft (15 m), and they are greater in the near-surface elements. This suggests that the cracks originate at the surface and then propagate downward. However, caliche-cemented alluvium is known to be present at a depth of about 5 ft (1.5 m) (Cordy et al., 1977). If Young's modulus of this rock-like material is high enough, the crack might be initiated at some shallow depth and then propagate both upward and downward.

REFERENCES

Bower, H., 1977, Land Subsidence and cracking due to a groundwater depletion: *Ground Water*, Vol. 15, No. 5, pp. 358–364.

Cordy, G. E.; Holway, J. V.; and Péwé, T. L., 1977, *Environmental Geology, Paradise Valley Quandrangle, Maricopa County, Arizona*, Unpublished Report: City of Scottsdale, Scottsdale, AZ, 14 maps, scale 1:24,000.

Desai, C. S. and Abel, J. F., 1972, *Introduction to the Finite Element Method:* Van Nostrand Reinhold, New York, NY, 477 p.

Lee, K. L. and Shen, C. K., 1969, Horizontal movements related to subsidence, In Proceedings, *Journal of the Soil Mechanics and Foundations Division, American Society of Civil Engineers*, Vol. 95, No. 1, pp. 139–166.

←

Figure 18. A) Displacements. The imposed vertical displacements which simulate the subsidence are shown along the lower left-hand edge of the section; where no vectors are shown, the nodes are completely constrained. The displacements at the surface due to the subsidence are shown along the top of the section; where they are not shown, the vectors are too short to plot. B) Stress distribution. The magnitude and orientation of the principal stresses in each element are shown by a scaled axial cross. The region of horizontal tension is outlined by a dotted line, and the magnitudes of the tensile stresses in the uppermost elements are shown graphically. C = the location of the actual crack, and P = the location of the predicted crack.

MAY 1986 VOLUME XXIII, NUMBER 2

BULLETIN OF THE ASSOCIATION OF ENGINEERING GEOLOGISTS

TABLE OF CONTENTS

101 **Geology of Johannesburg, Republic of South Africa** . . . . . Johannes H. De Beer

139 **Origin of Land Subsidence and Earth Fissuring, Northeast Phoenix, Arizona** . . . . . Michael K. Larson and Troy L. Péwé

167 **SSNAP 3D: Shearing Response along Rough Fractures: Part 1—Theoretical Considerations** . . . . . Norbert R. P. Baczynski

181 **SSNAP 3D: Shearing Response along Rough Fractures: Part 2—Field Application** . . Norbert R. P. Baczynski, Donald R. Willoughby, and Colin C. McBurney

197 **Effects of the 1906 Earthquake on the Bald Hill Outlet System, San Mateo County, California** . . . . . Earl H. Pampeyan

209 **The Long Journey from Discovery to Clean-Up of Superfund Sites** . . . . . Yane Nordhav, Greg Shepherd, and Karen L. O'Regan

215 **Memorial to Robert M. Lindvall (1916-1985)** . . . . . Richard W. Lemke